High Order Discontinuous Galerkin Methods for Fluid and Solid Mechanics

Per-Olof Persson

Department of Mathematics
Massachusetts Institute of Technology

Collaborators: J. Peraire, J. Bonet, M. Drela, D. J. Willis,
N. C. Nguyen, E. Israeli, A. Uranga, A. Mohnot, J. P. Whitney

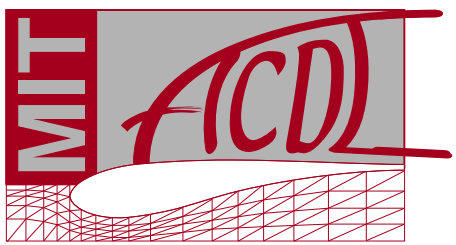

Department of Aeronautics & Astronautics
Massachusetts Institute of Technology
March 19, 2008

Outline

1. Introduction
2. Discretization and Solvers
   - High-Order Mesh Generation
   - The Discontinuous Galerkin Method
   - The Compact Discontinuous Galerkin (CDG) Method
   - Preconditioning for Newton-Krylov Solvers
   - Stabilization with Artificial Viscosity
3. Deformable Domains
   - Mapping-based ALE Formulation
   - Flapping Flight Applications
4. Large Deformation Solid Dynamics
   - High-Order Lagrangian DG Formulations
   - Applications: Thin structures, viscoplasticity
5. Conclusions

Motivation

- Need for higher fidelity predictions in computational mechanics
  - DNS/LES/DES applications
  - Accurate RANS for engineering applications (drag prediction, rotor dynamics, fluid/structure interaction, flapping flight)
  - Computational aeroacoustics (direct solution of compressible flow, accurate computation of noise sources)
  - Other problems involving wave propagation, multiple scale phenomena, and non-linear interactions

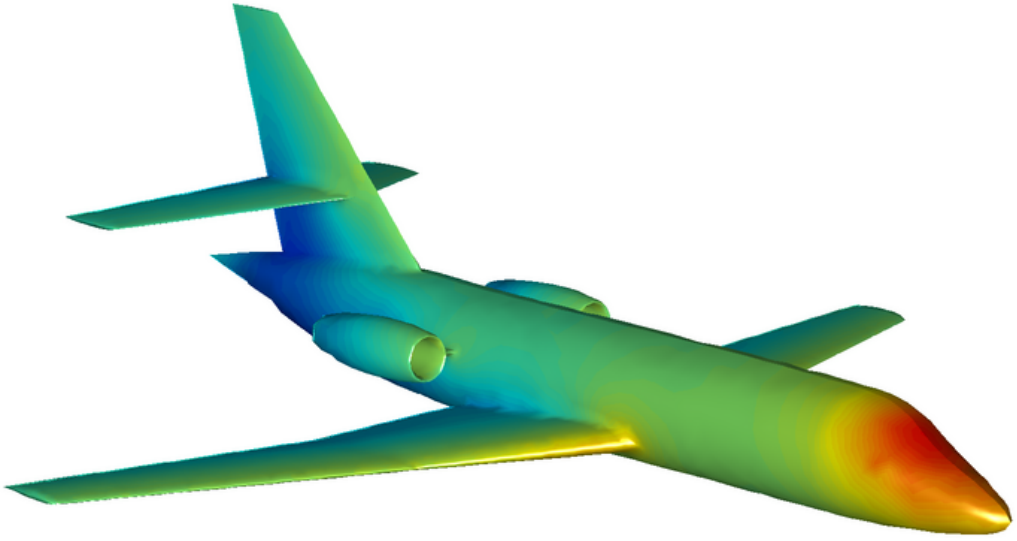

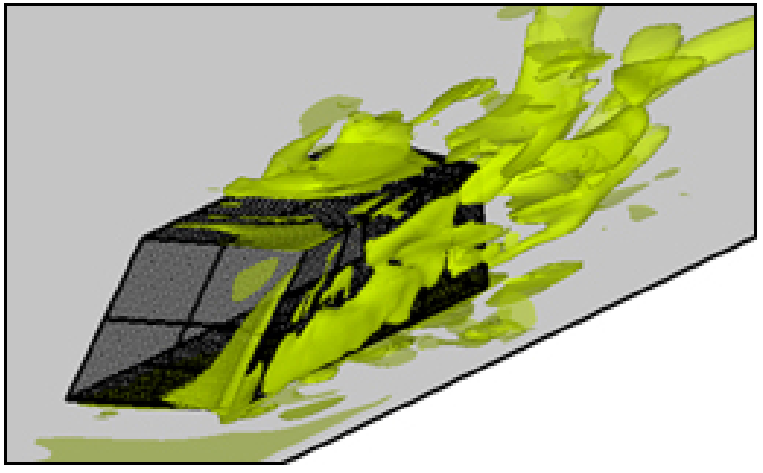

Example: Wave propagation

- Scalar convection equation $u_t + u_x = 0$, fixed resolution

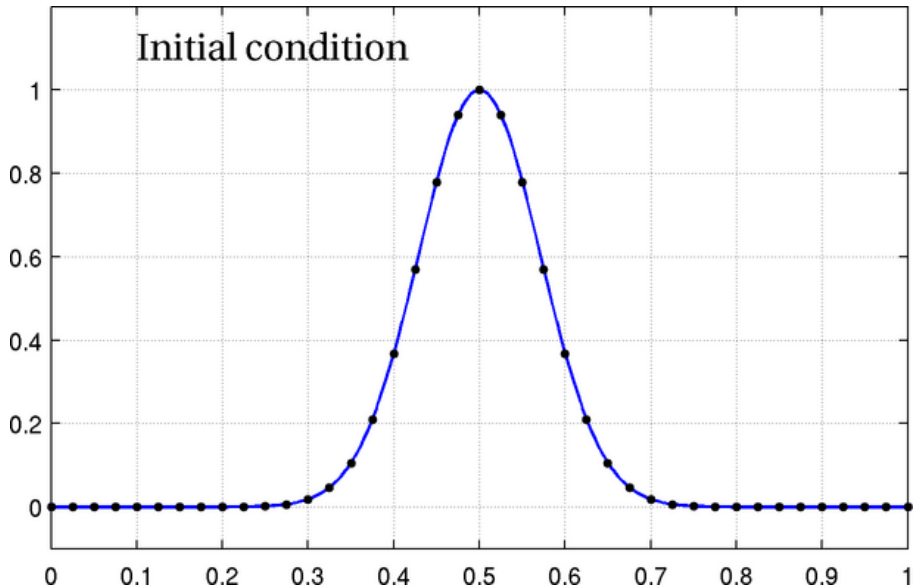

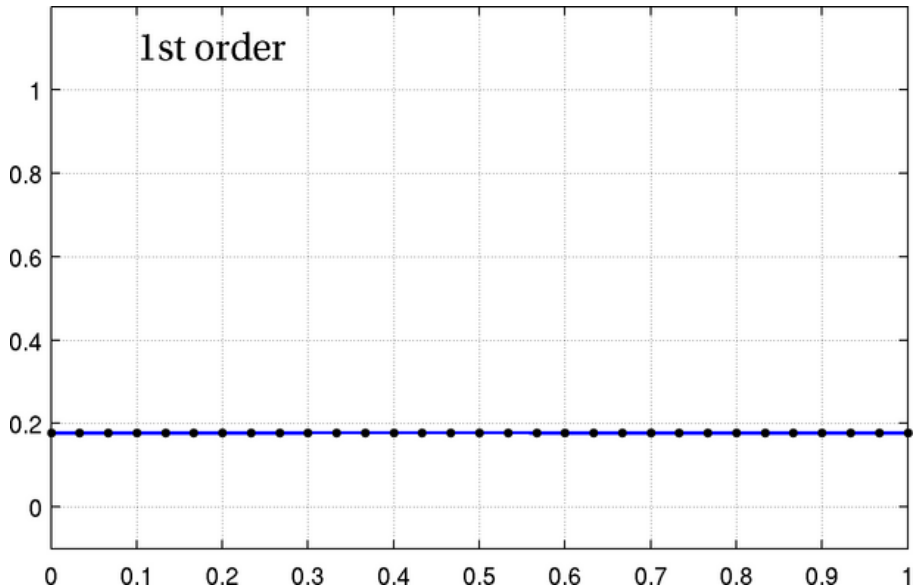

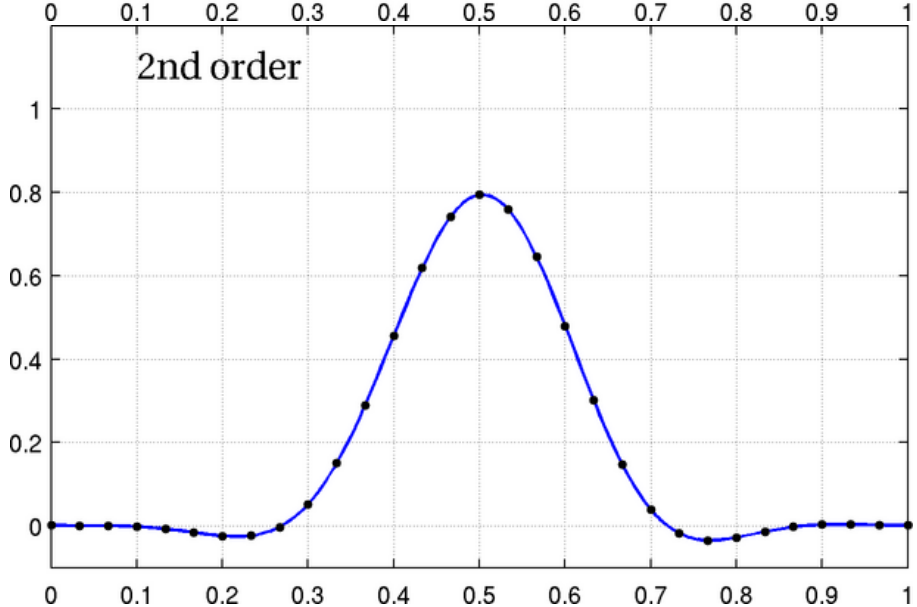

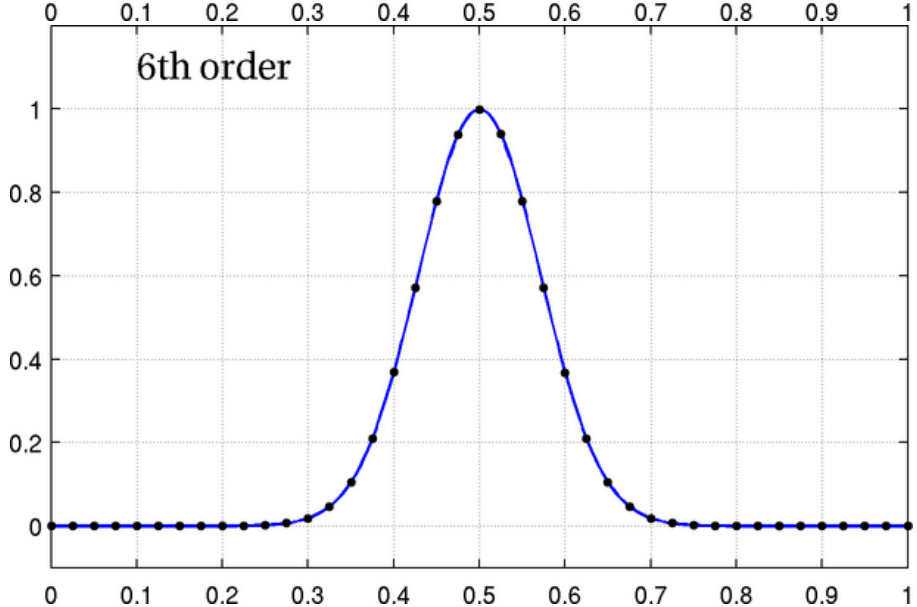

Example: Aeroacoustics and K-H Instability

- Inspired by calculations of Munz et al [03] (linearized)
- Nonlinear behavior: Large scale acoustic wave interacts with small scale flow features, leading to vorticity generation
- $p = 7$ (8th order accuracy), 140-by-28 square elements

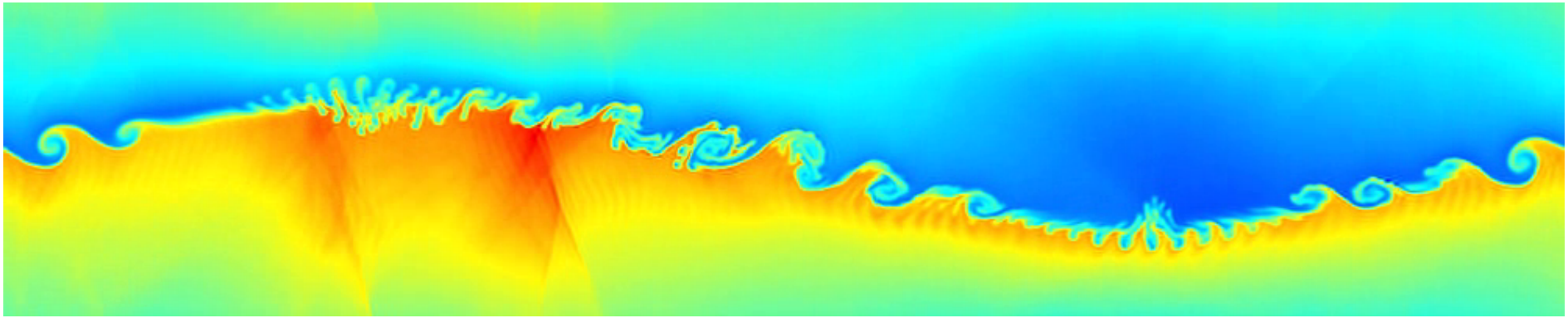

Failure of Low-Order Methods

- From the third Drag Prediction Workshop (DPW), June 2006:

"...the dominant sources of error in aerodynamic drag prediction are related to spatial discretization error..."

"...the collective workshop results have not demonstrated substantially reduced variability ... in spite of over an order of magnitude increase in grid resolution from the first to the third workshop."

"...the demonstration of apparent grid convergence is contradicted by results obtained with the same code on grids of different construction."

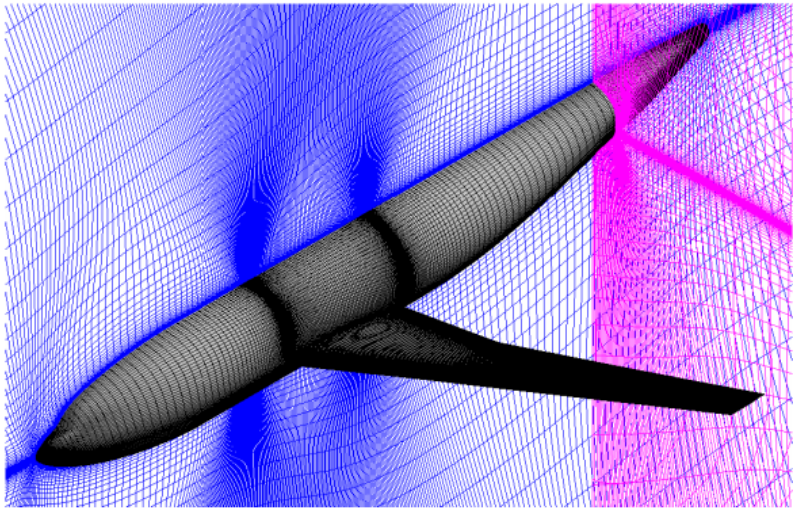

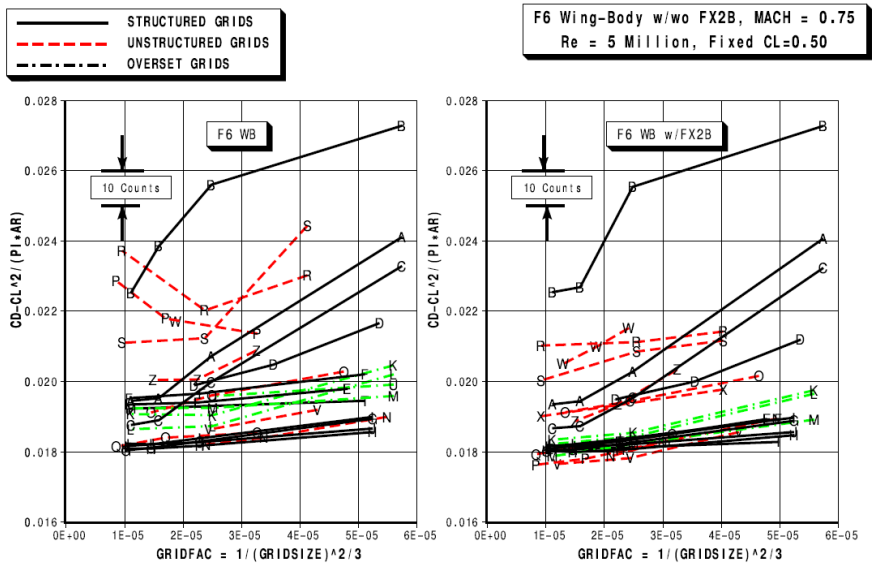

Motivation

- Fundamental properties of Discontinuous Galerkin (DG) methods:

	FVM	FDM	FEM	DG
1) High-order/Low dispersion	✗	✓	✓	✓
2) Unstructured meshes	✓	✗	✓	✓
3) Stability for conservation laws	✓	✓	✗	✓

- However, several problems to resolve:
  - High CPU/memory requirements (compared to FVM or H-O FDM)
  - Low tolerance to under-resolved features
  - High-order geometry representation and mesh generation
- *The challenge is to make DG competitive for real-world problems*

Outline

1. Introduction
2. Discretization and Solvers
   - High-Order Mesh Generation
   - The Discontinuous Galerkin Method
   - The Compact Discontinuous Galerkin (CDG) Method
   - Preconditioning for Newton-Krylov Solvers
   - Stabilization with Artificial Viscosity
3. Deformable Domains
   - Mapping-based ALE Formulation
   - Flapping Flight Applications
4. Large Deformation Solid Dynamics
   - High-Order Lagrangian DG Formulations
   - Applications: Thin structures, viscoplasticity
5. Conclusions

Mesh Generation for Complex Geometries

Unstructured meshes *required for realistic problems*

- Geometric and adaptive flexibility, accurate boundary treatment
- Tetrahedral meshes give robustness and automation

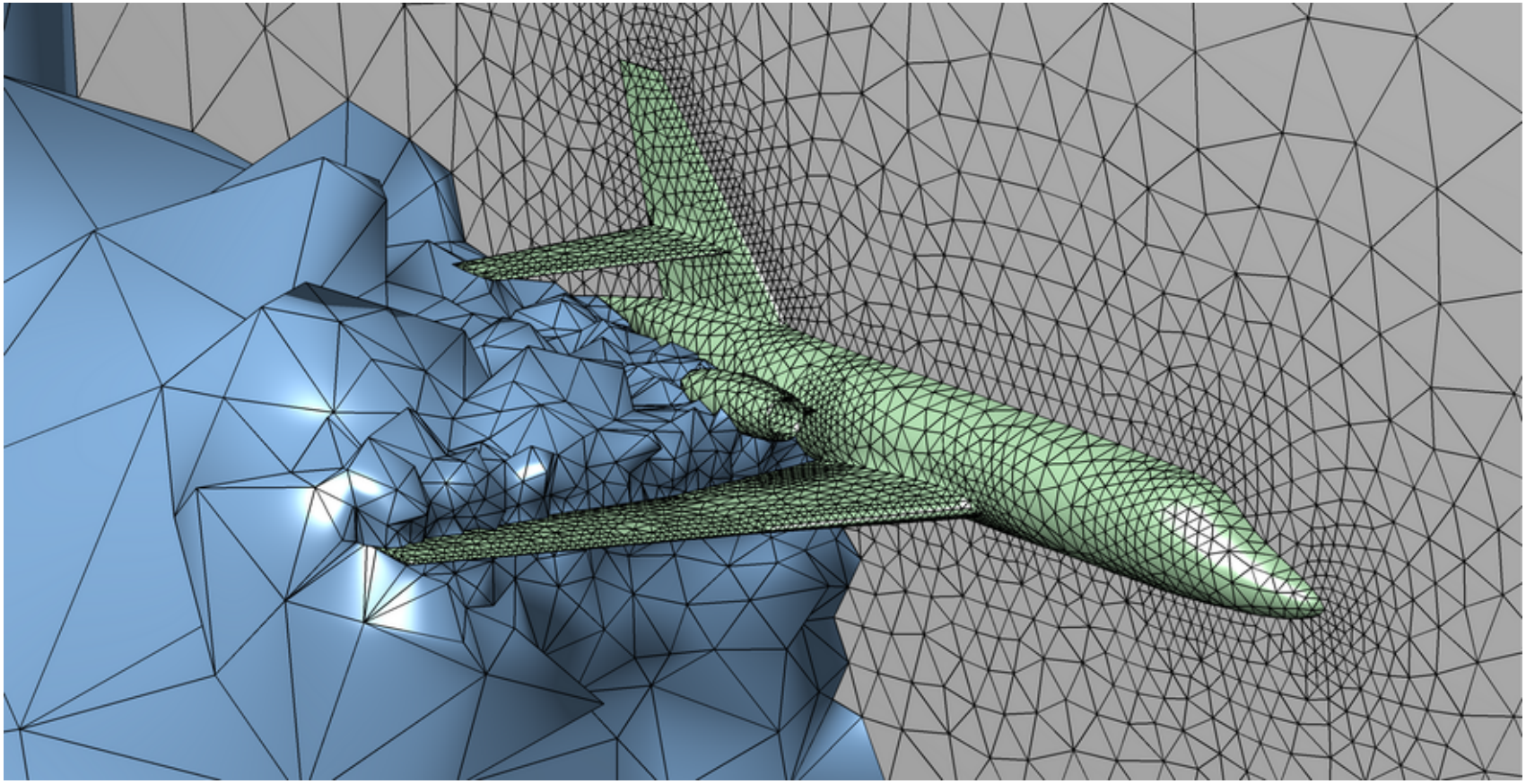

Example: Flow around Elliptic Wing

- Computational efficiency by resolving relevant flow features

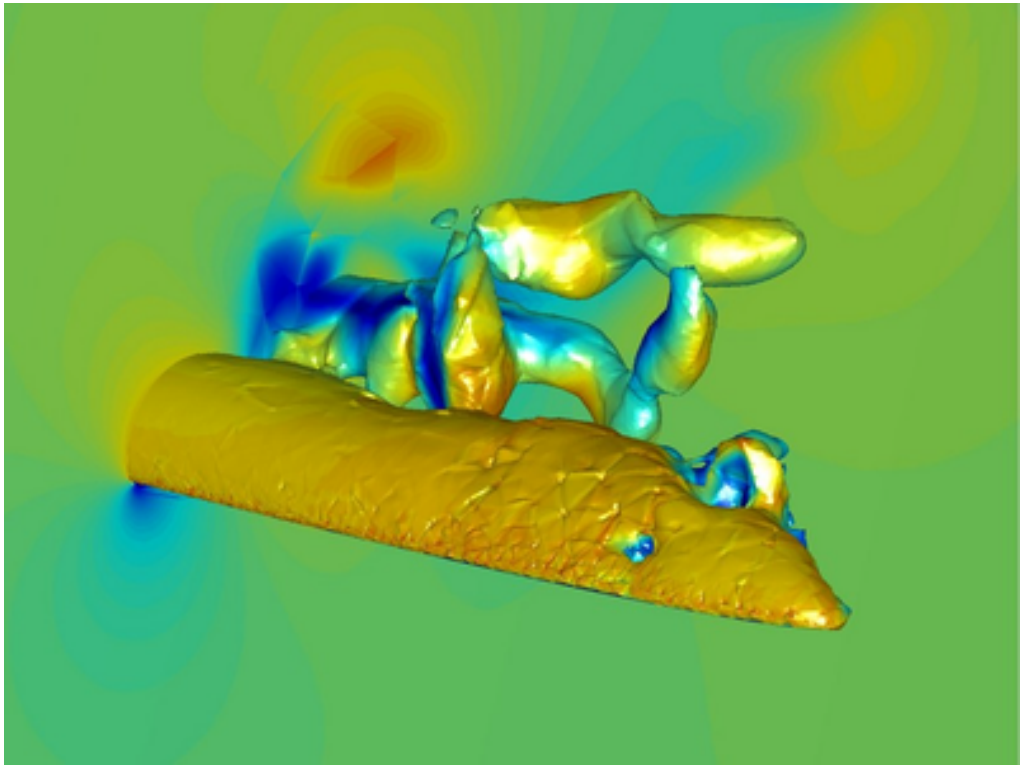

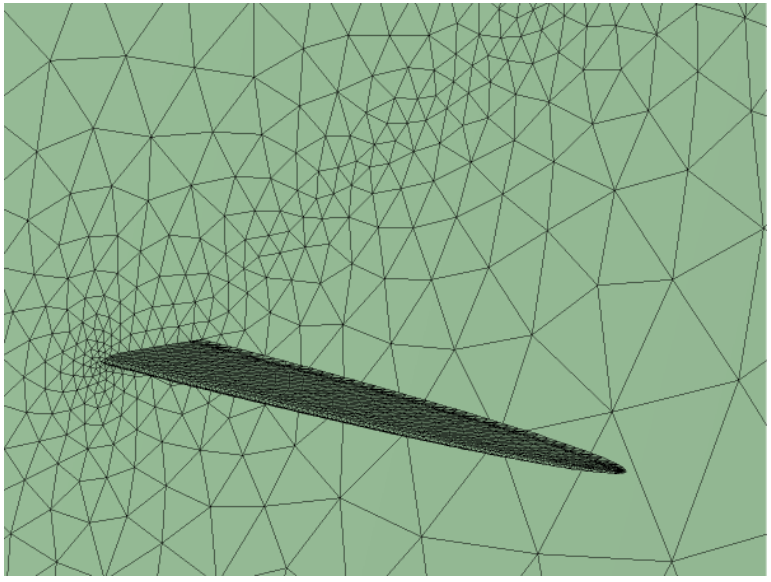

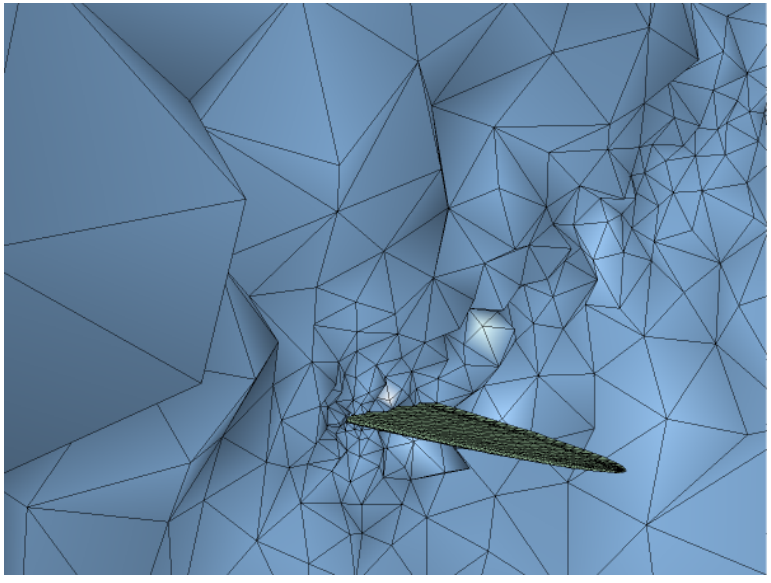

The DistMesh Mesh Generator

- High quality meshes obtained using the *DistMesh* algorithm [Persson Ph.D. thesis, 2005]
  1. Start with *any* topologically correct initial mesh, for example random node distribution and Delaunay triangulation
  2. Move nodes to find force equilibrium in edges
     - Project boundary nodes using *implicit geometry* $\phi(\boldsymbol{x})$
     - Update element connectivities with Delaunay

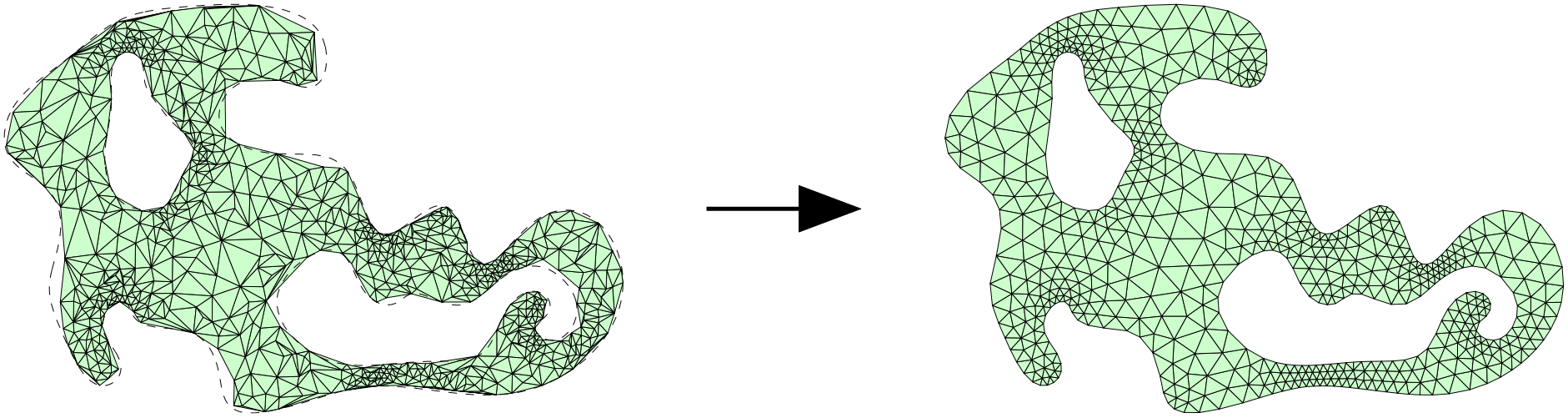

DistMesh Applications

- High quality meshes from images and MRI/CT scans

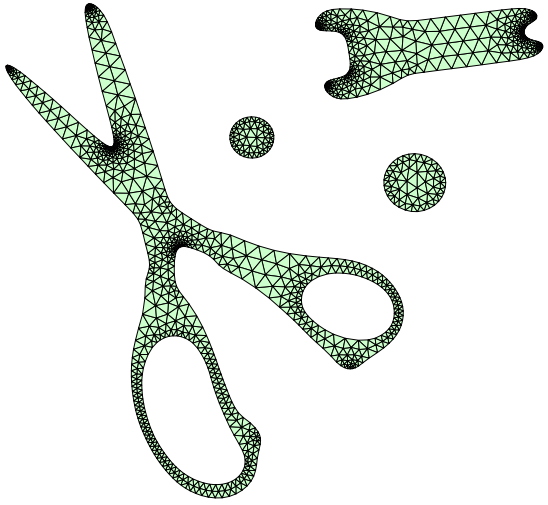

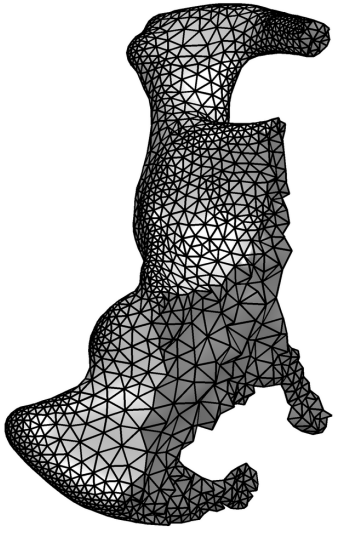

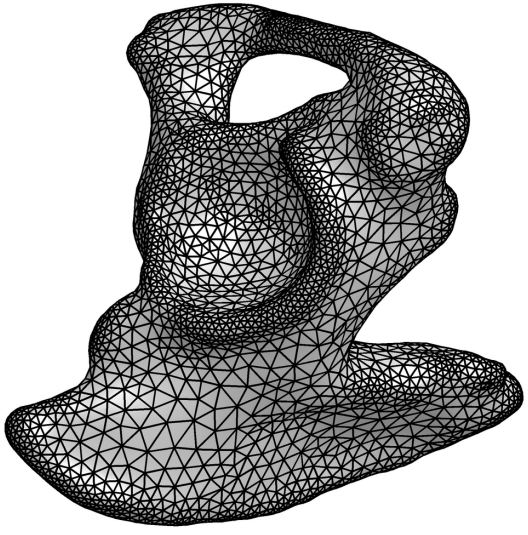

DistMesh Applications

- Shape optimization by combined levelset/finite element method

Structural design (compliance minimization)

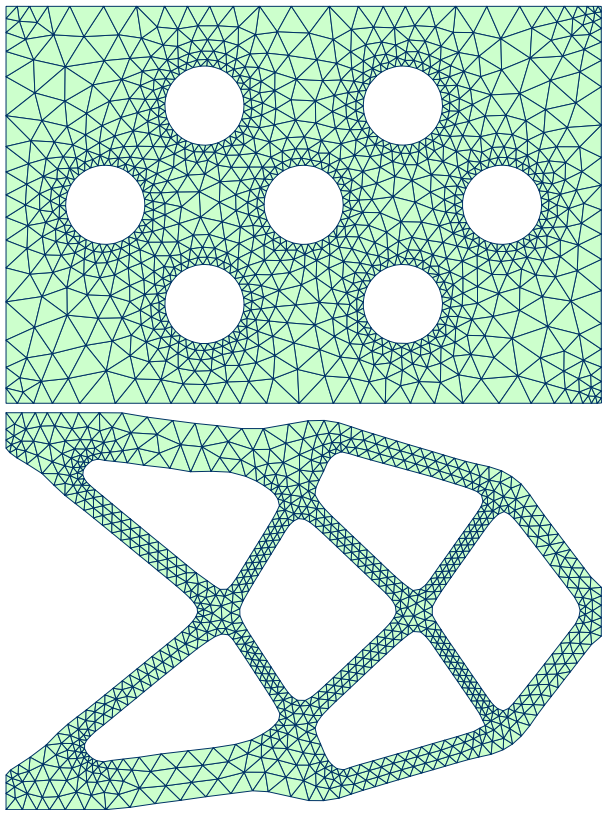

Vibration control (eigenvalue minimization)

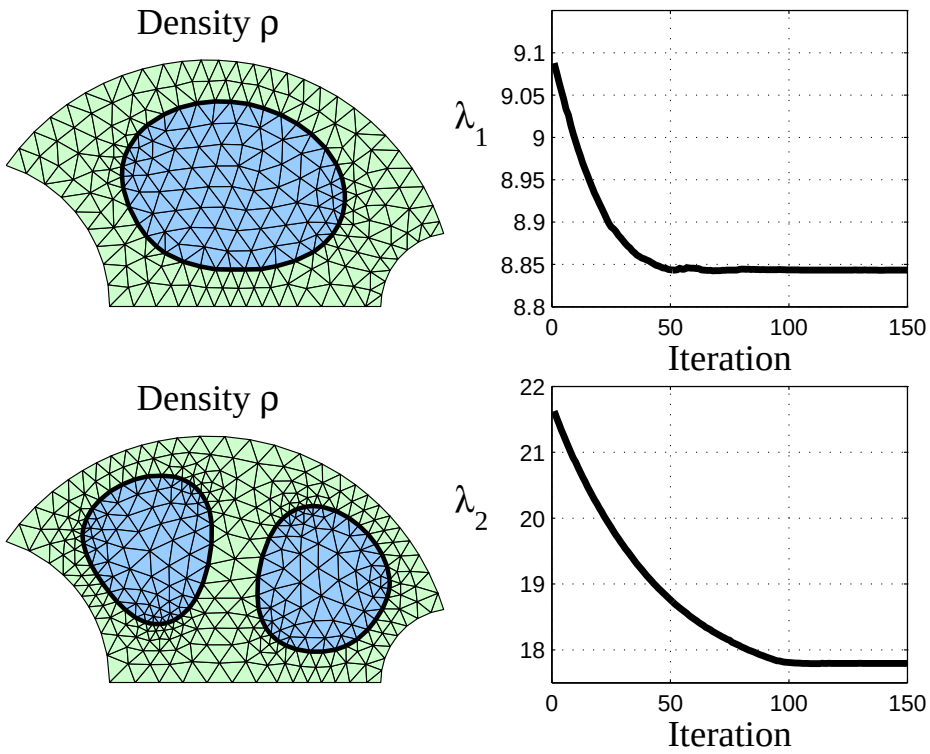

High-Order Curved Mesh Generation

- Open research topic: Unstructured curved mesh generation
- High quality meshes make it easier to avoid inversion
- DistMesh approach for automatic curving (ongoing work)

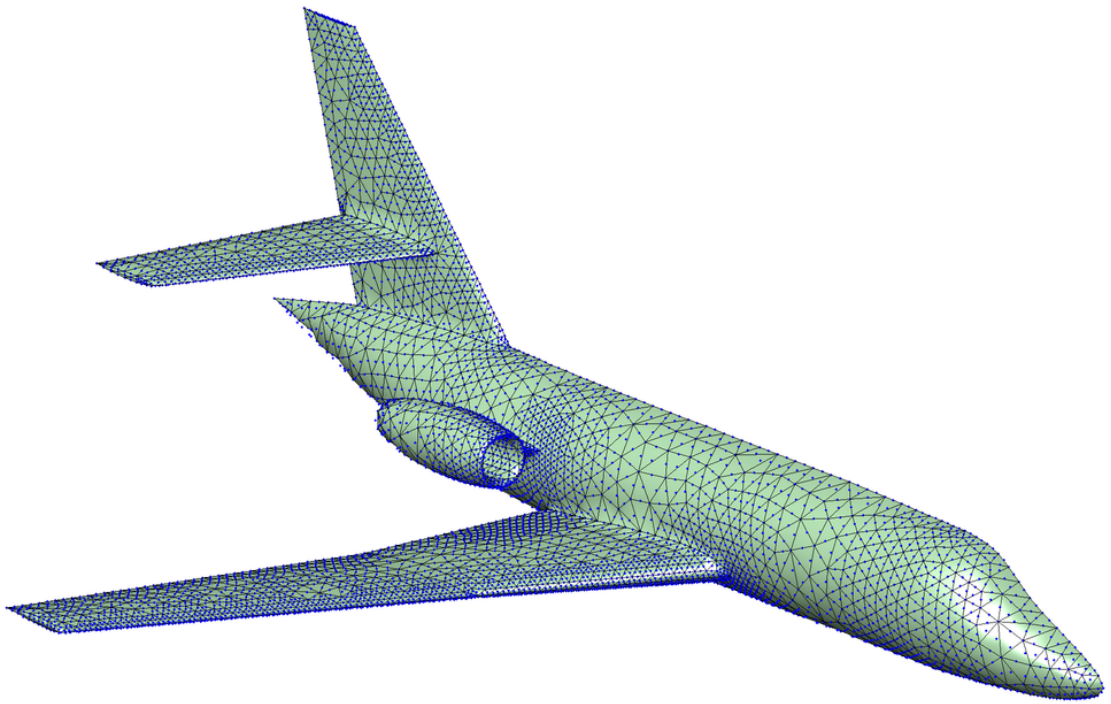

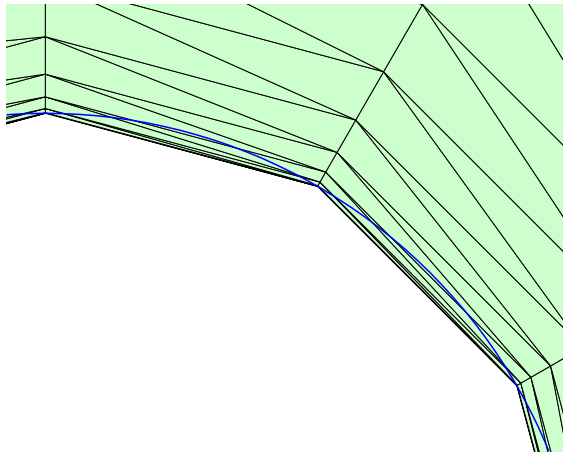

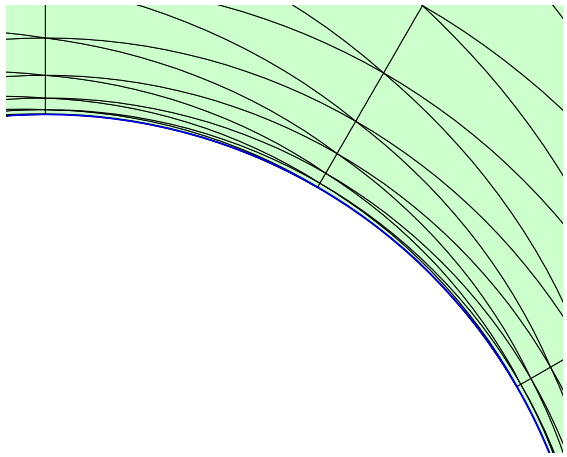

Outline

1. Introduction
2. Discretization and Solvers
   - High-Order Mesh Generation
   - The Discontinuous Galerkin Method
   - The Compact Discontinuous Galerkin (CDG) Method
   - Preconditioning for Newton-Krylov Solvers
   - Stabilization with Artificial Viscosity
3. Deformable Domains
   - Mapping-based ALE Formulation
   - Flapping Flight Applications
4. Large Deformation Solid Dynamics
   - High-Order Lagrangian DG Formulations
   - Applications: Thin structures, viscoplasticity
5. Conclusions

The Discontinuous Galerkin Method

- (Reed/Hill 1973, Lesaint/Raviart 1974, Cockburn/Shu 1989-, etc)
- Consider non-linear hyperbolic system in conservative form:

$$\boldsymbol{u}_t + \nabla \cdot \mathcal{F}_i(\boldsymbol{u}) = 0$$

- Triangulate domain Ω into elements $\kappa \in T_h$
- Seek approximate solution $\boldsymbol{u}_h$ in space of element-wise polynomials:

$$\mathcal{V}_h^p = \{\boldsymbol{v} \in L^2(\Omega) : \boldsymbol{v}|_\kappa \in P^p(\kappa)\ \forall \kappa \in T_h\}$$

- Multiply by test function $\boldsymbol{v}_h \in \mathcal{V}_h^p$ and integrate over element κ:

$$\int_\kappa \left[(\boldsymbol{u}_h)_t + \nabla \cdot \mathcal{F}_i(\boldsymbol{u}_h)\right] \boldsymbol{v}_h \, d\boldsymbol{x} = 0$$

The Discontinuous Galerkin Method

- Integrate by parts:

$$\int_\kappa [(\boldsymbol{u}_h)_t]\, \boldsymbol{v}_h \, d\boldsymbol{x} - \int_\kappa \mathcal{F}_i(\boldsymbol{u}_h) \nabla \boldsymbol{v}_h \, d\boldsymbol{x} + \int_{\partial\kappa} \hat{\mathcal{F}}_i(\boldsymbol{u}_h^+, \boldsymbol{u}_h^-, \hat{\boldsymbol{n}}) \boldsymbol{v}_h^+ \, ds = 0$$

  with numerical flux function $\hat{\mathcal{F}}_i(\boldsymbol{u}_L, \boldsymbol{u}_R, \hat{\boldsymbol{n}})$ for left/right states $\boldsymbol{u}_L$,$\boldsymbol{u}_R$ in direction $\hat{\boldsymbol{n}}$ (Godunov, Roe, Osher, Van Leer, Lax-Friedrichs, etc)

- Global problem: Find $\boldsymbol{u}_h \in \mathcal{V}_h^p$ such that this weighted residual is zero for all $\boldsymbol{v}_h \in \mathcal{V}_h^p$
- Error $= \mathcal{O}(h^{p+1})$ for smooth solutions

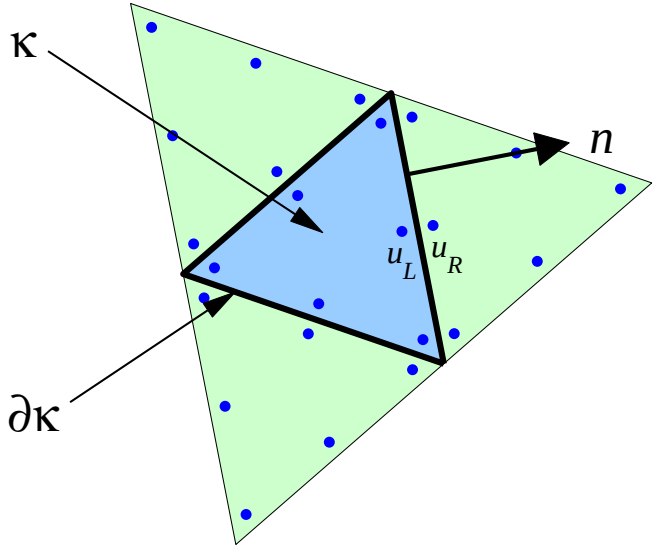

The DG Method – Observations

- Reduces to the finite volume method for $p = 0$:

$$(\boldsymbol{u}_h)_t A_\kappa + \int_{\partial\kappa} \hat{\mathcal{F}}_i(\boldsymbol{u}_h^+, \boldsymbol{u}_h^-, \hat{\boldsymbol{n}})\, ds = 0$$

- Boundary conditions enforced naturally for any degree p
- Block-diagonal mass matrix (no overlap between basis functions)
- Block-wise compact stencil – neighboring elements connected

Mass Matrix

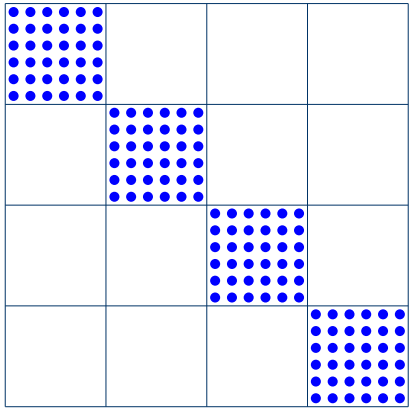

Jacobian

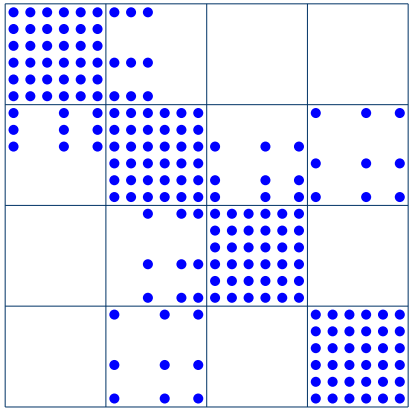

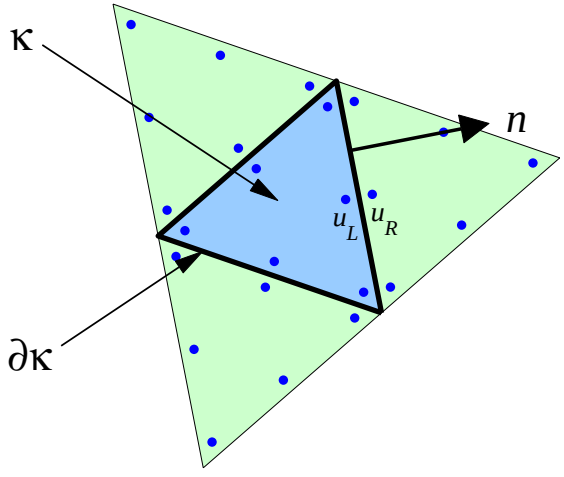

Outline

1. Introduction
2. Discretization and Solvers
   - High-Order Mesh Generation
   - The Discontinuous Galerkin Method
   - The Compact Discontinuous Galerkin (CDG) Method
   - Preconditioning for Newton-Krylov Solvers
   - Stabilization with Artificial Viscosity
3. Deformable Domains
   - Mapping-based ALE Formulation
   - Flapping Flight Applications
4. Large Deformation Solid Dynamics
   - High-Order Lagrangian DG Formulations
   - Applications: Thin structures, viscoplasticity
5. Conclusions

Viscous Discretization

- General approach for second derivatives:
  - Write as system of first order equations:

$$\boldsymbol{u}_t + \nabla \cdot \mathcal{F}_i(\boldsymbol{u}) - \nabla \cdot \mathcal{F}_v(\boldsymbol{u}, \boldsymbol{\sigma}) = 0$$

$$\boldsymbol{\sigma} - \nabla \boldsymbol{u} = 0$$

  - Discretize using DG, choose appropriate numerical fluxes $\hat{\sigma}$, $\hat{u}$
- Various schemes have been proposed:
  - *BR1* [Bassi/Rebay 97]: Averaging, unstable and non-compact
  - *BR2* [Bassi/Rebay 98]: Different lifting operator for each edge, compact connectivities, similar to Interior Penalty (IP)
  - *LDG* [Cockburn/Shu 98]: Upwind/Downwind, non-compact
  - *CDG* [Peraire/Persson 07]:
    Modification of LDG for local dependence – sparse and compact

The Local DG Method

- Consider Poisson problem $-\nabla \cdot (\kappa \nabla u) = f$
- Write as system of first order equations,

$$-\nabla \cdot \boldsymbol{\sigma} = f$$

$$\boldsymbol{\sigma} = \kappa \nabla u$$

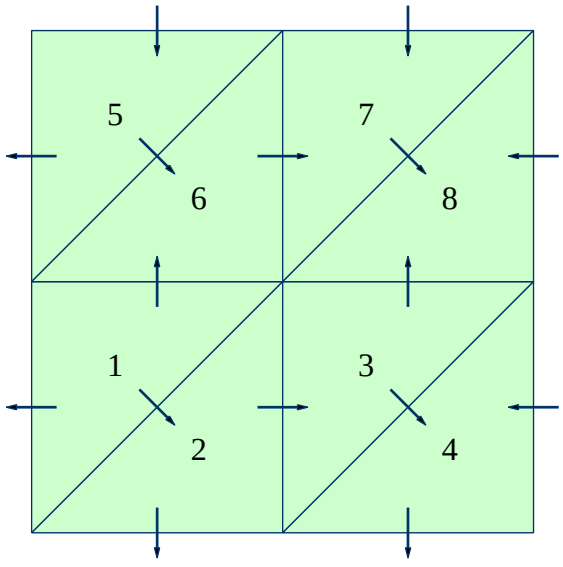

- Use numerical inter-element fluxes

$$\hat{\boldsymbol{\sigma}} = \{\boldsymbol{\sigma}_h\} - C_{11}[u_h] + \boldsymbol{C}_{12}[\boldsymbol{\sigma}_h]$$

$$\hat{u} = \{u_h\} - \boldsymbol{C}_{12} \cdot [u_h]$$

where $\{\cdot\}, [\cdot]$ denote averaging and difference

- In particular, choosing $\boldsymbol{C}_{12} = 1$ or -1 depending on a *switch* for each edge, will upwind/downwind $\hat{\boldsymbol{\sigma}}, \hat{u}$

The Local DG Scheme

- Solving for the variables $\boldsymbol{\sigma}_h$ gives

$$\boldsymbol{\sigma}_h = \kappa \nabla_h u_h + \bar{\boldsymbol{\sigma}}_h$$

where

$$\bar{\boldsymbol{\sigma}}_h = \kappa r([u_h]) + \kappa l(\boldsymbol{C}_{12} \cdot [u_h]) + \text{ boundary terms}$$

and $r(\phi)$ and $l(q)$ are *lifting operators* (essentially L_2-projections)

- In general, this introduces non-local couplings since the lifting operators involve all element edges

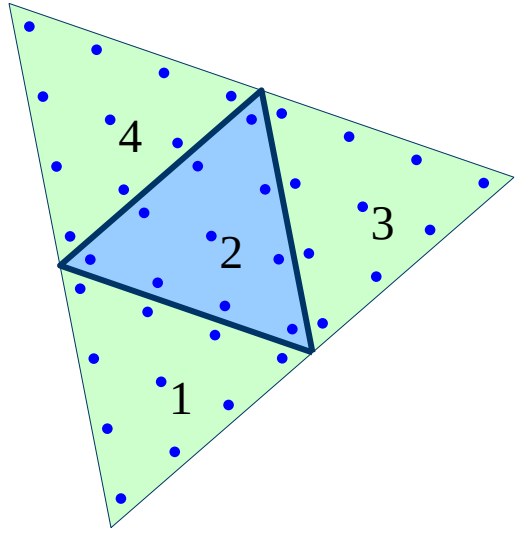

The Compact DG Scheme

- In the CDG scheme, we split the lifting operators into sums of edge-wise lifting operators $r^e(\phi)$, $l^e(q)$, and set

$$\hat{\boldsymbol{\sigma}} = \{\boldsymbol{\sigma}_h^e\} - C_{11}[u_h] + \boldsymbol{C}_{12}[\boldsymbol{\sigma}_h^e]$$

$$\hat{u} = \{u_h\} - \boldsymbol{C}_{12} \cdot [u_h]$$

  where $\boldsymbol{\sigma}_h^e = \kappa \nabla_h u_h + \bar{\boldsymbol{\sigma}}_h^e$, with

$$\bar{\boldsymbol{\sigma}}_h^e = \kappa r^e([u_h]) + \kappa l^e(\boldsymbol{C}_{12} \cdot [u_h]) + \text{ boundary terms}$$

- Since only the lifting operator corresponding to the current edge is used, only neighboring elements are connected

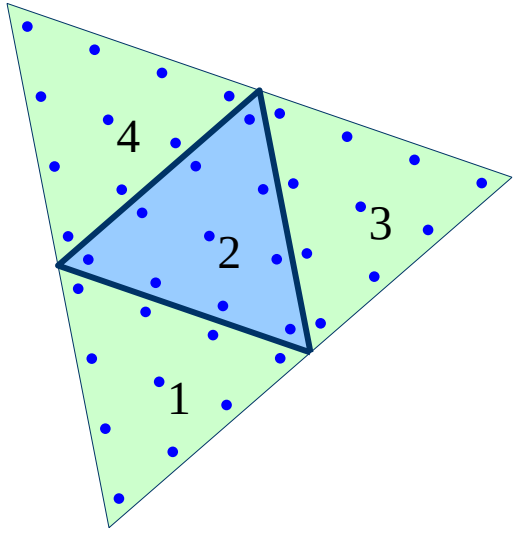

Error Estimates

- In primal form, the LDG scheme becomes (ignoring bnd terms):

$$\int_\Omega \kappa(r([u]) + l(\boldsymbol{C}_{12} \cdot [u])) \cdot (r([v]) + l(\boldsymbol{C}_{12} \cdot [v]))\, dx =$$
$$\sum_{e \in \mathcal{E}_i} \sum_{f \in \mathcal{E}_i} \int_\Omega \kappa(r^e([u]) + l^e(\boldsymbol{C}_{12} \cdot [u])) \cdot (r^f([v]) + l^f(\boldsymbol{C}_{12} \cdot [v]))\, dx$$

- The CDG scheme excludes some terms that are indefinite:

$$\sum_{e \in \mathcal{E}_i} \int_\Omega \kappa(r^e([u]) + l^e(\boldsymbol{C}_{12} \cdot [u])) \cdot (r^e([v]) + l^e(\boldsymbol{C}_{12} \cdot [v]))\, dx =$$
$$\sum_{e \in \mathcal{E}_i} \sum_{f \in \mathcal{E}_i} \delta_{ef} \int_\Omega \kappa(r^e([u]) + l^e(\boldsymbol{C}_{12} \cdot [u])) \cdot (r^f([v]) + l^f(\boldsymbol{C}_{12} \cdot [v]))\, dx$$

- Non-compact terms are eliminated but the scheme remains stable

Error Estimates

- Coercivity and boundedness for the CDG scheme same as for LDG, leading to a-*priori* estimates:

$$|||u - u_h||| \leq Ch^p |u|_{p+1,\Omega}$$

and

$$||u - u_h||_{0,\Omega} \leq Ch^{p+1} |u|_{p+1,\Omega}$$

with the norm

$$|||v|||^2 = \sum_{K \in \mathcal{T}_h} |v|^2_{1,K} + \sum_{e \in \mathcal{E}_i} ||r_e([v])||^2_{0,\Omega} + \sum_{e \in \partial\Omega_D} ||r_D(v)||^2_{0,\Omega}$$

- Assumes $C_{11} = \mathcal{O}(h^{-1})$, but is observed numerically for $C_{11} = 0$

The CDG Method – Summary

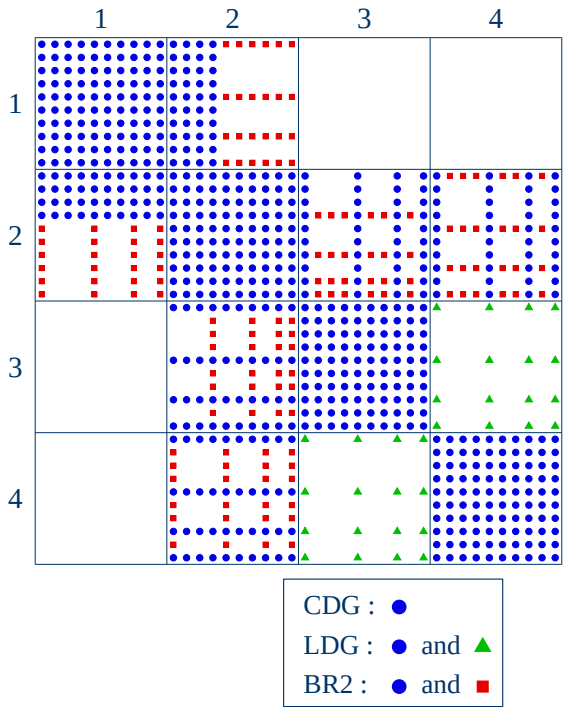

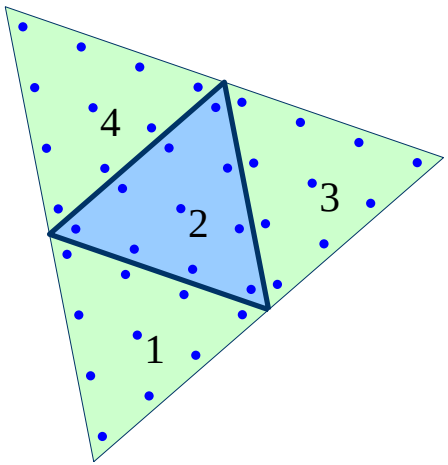

- Modification of numerical fluxes in LDG scheme
- Excludes non-compact and indefinite terms
- Provably optimal accuracy $\mathcal{O}(h^{p+1})$
- Higher stability/accuracy than LDG/BR2
- Sparser than LDG/BR2/IP

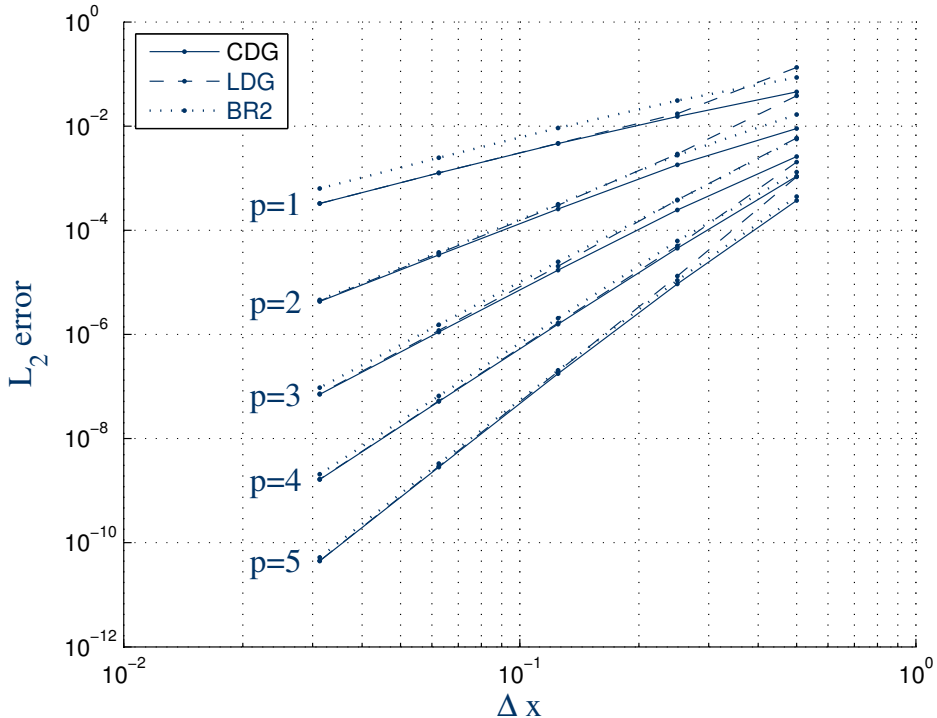

Switches and Null-space Dimensions

- Unlike the LDG scheme, the CDG scheme appears to be stable for $C_{11} = 0$ and an *inconsistent switch* such as highest element number
- Simple test [Sherwin et al 05]: Poisson problem, periodic boundary conditions, expected nullspace dimension = 1

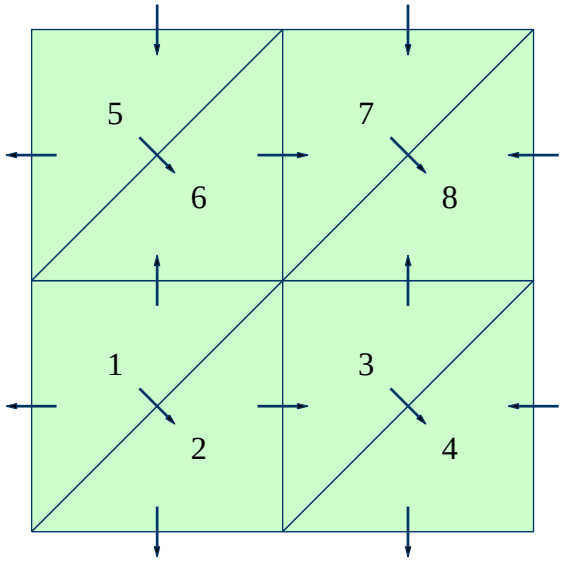

Nullspace dimension

Polynomial order p		1	2	3	4	5	6	7
Consistent switch	CDG	1	1	1	1	1	1	1
	LDG	1	1	1	1	1	1	1
Natural switch	CDG	1	1	1	1	1	1	1
	LDG	3	4	5	6	7	8	9

ILU and Switch Orientation

- Orientation of lower-triangular blocks important for ILU sparsity
- Take advantage of CDG's insensitivity to orientation

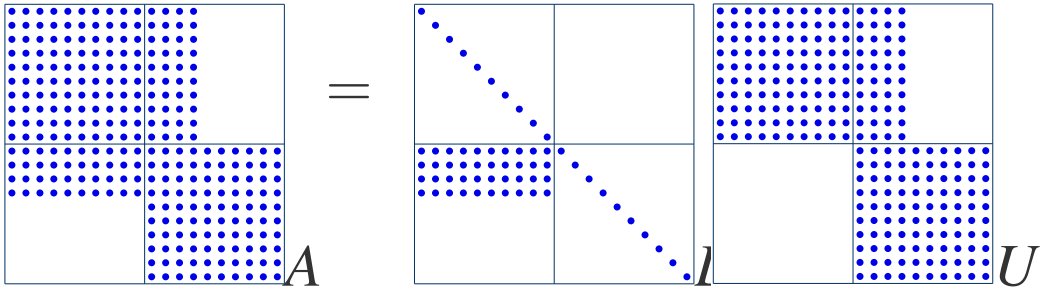

Switch 1:

Same LU storage

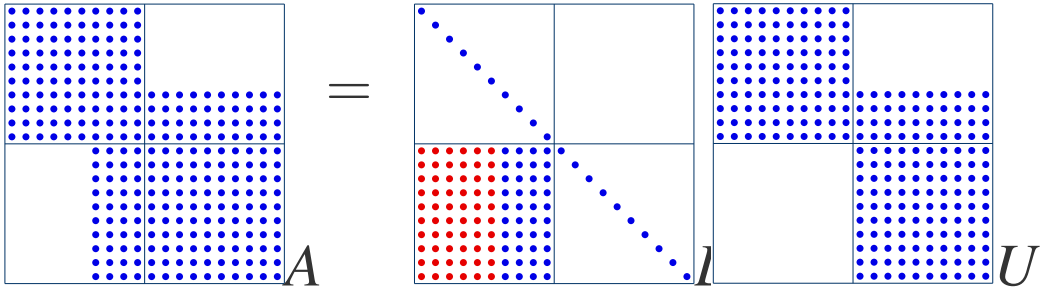

Switch 2:

More LU storage

Switches and Null-space Dimensions

- No additional non-zeros in block-ILU(0) factorization using CDG
- Dense lower-triangular blocks using BR2 / IP

CDG

Stiffness Matrix

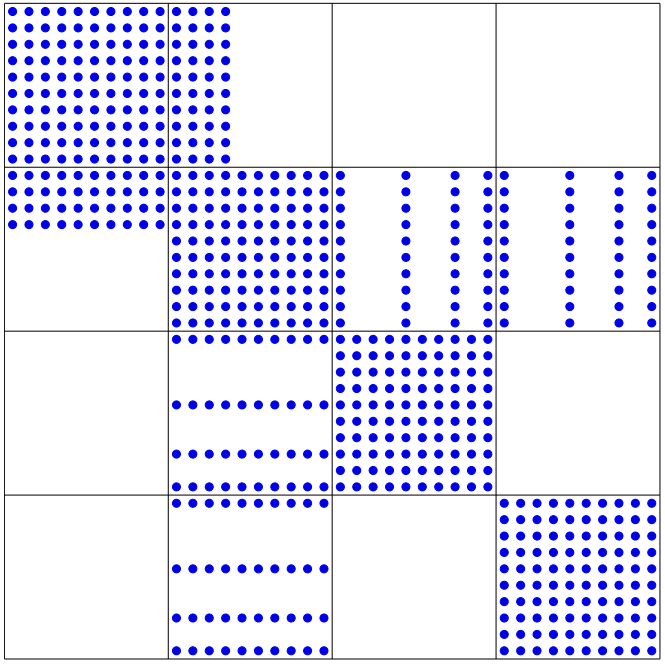

640 non-zeros

Block ILU(0)

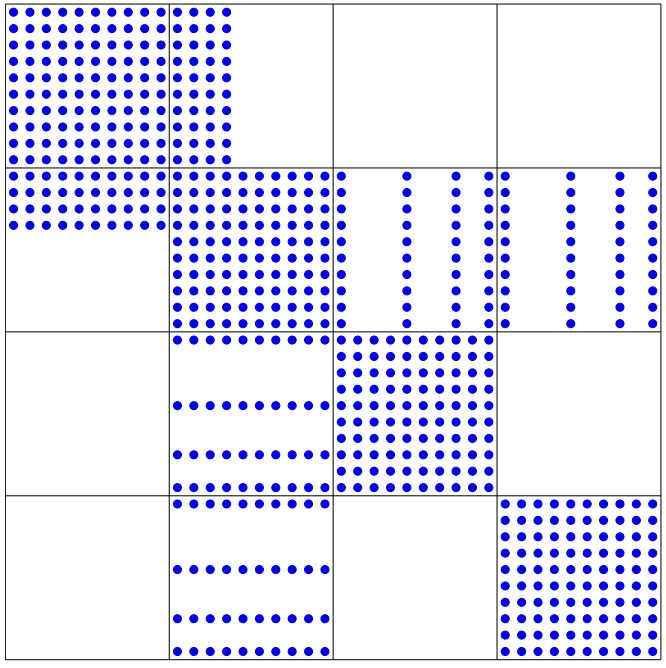

640 non-zeros

Switches and Null-space Dimensions

- No additional non-zeros in block-ILU(0) factorization using CDG
- Dense lower-triangular blocks using BR2 / IP

BR2 / IP

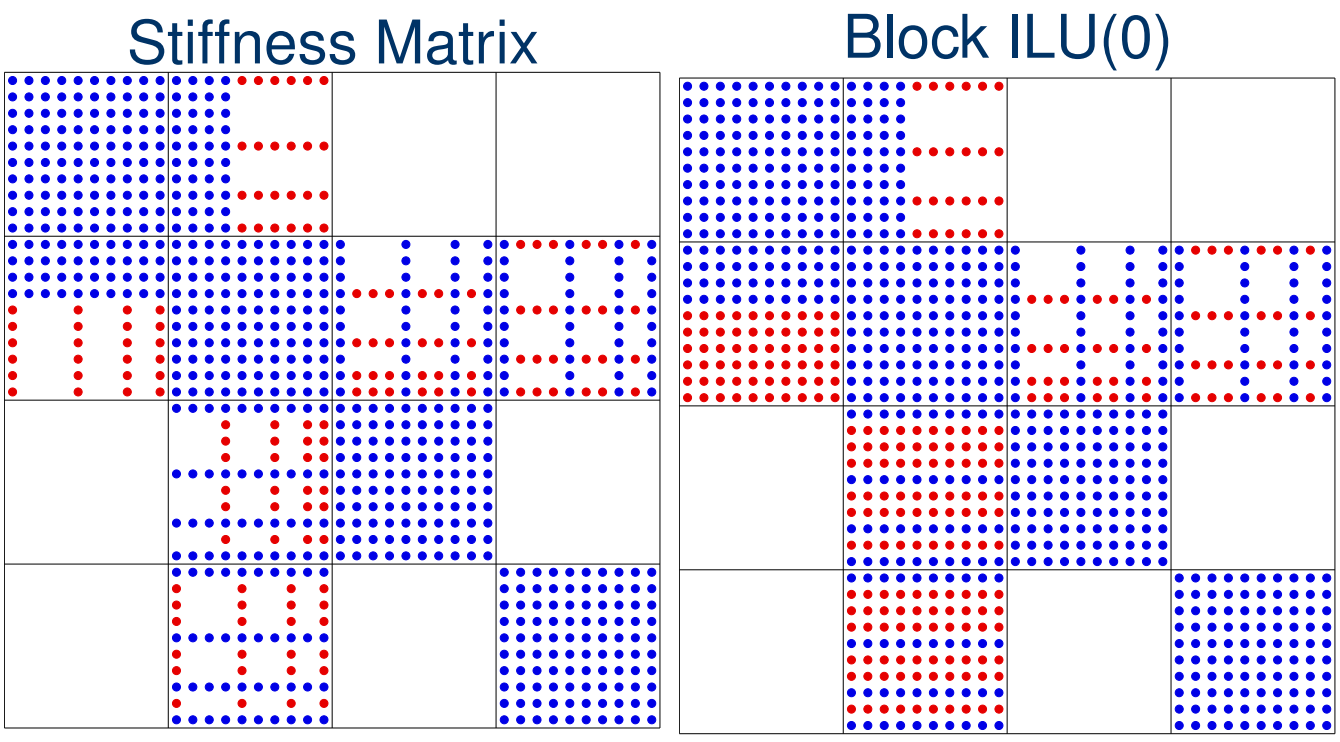

Matrix Representation

- Block matrix representation *fundamental for high performance*
  - Solver algorithms based on blocks
  - Up to 10 times higher performance with optimized BLAS
- Compact stencil $\Longrightarrow$ Matrix structure given by mesh connectivities
- Hard to store LDG/BR2/IP efficiently

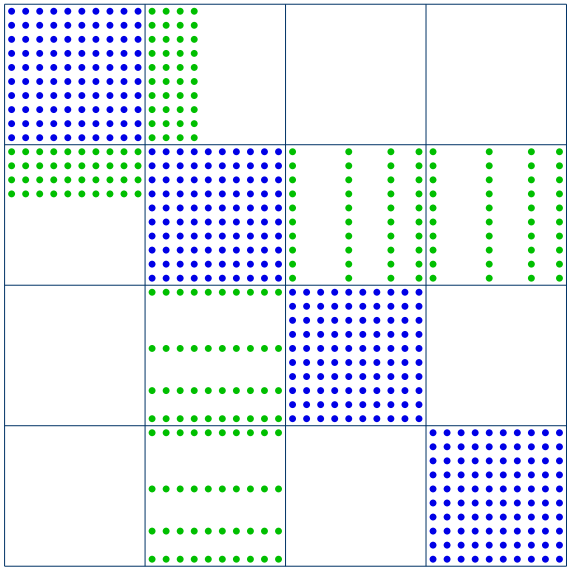

CDG – 2 arrays

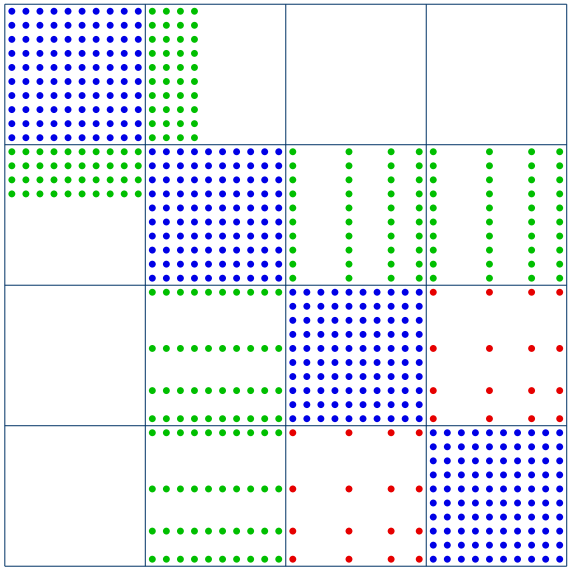

LDG – 3 arrays + struct

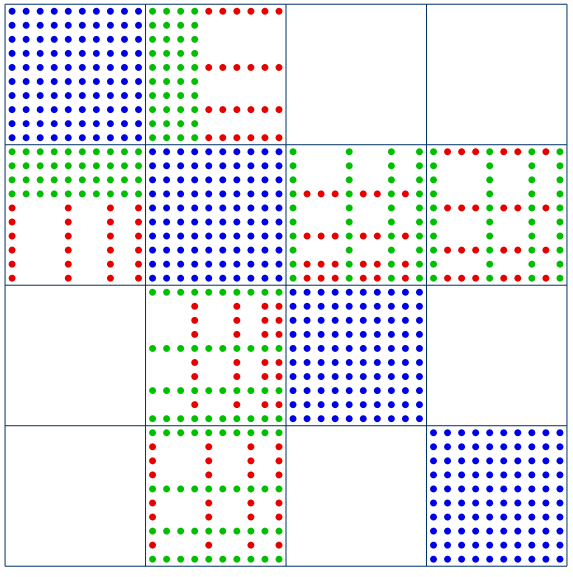

BR2 / IP – 3 arrays

Outline

1. Introduction
2. Discretization and Solvers
   - High-Order Mesh Generation
   - The Discontinuous Galerkin Method
   - The Compact Discontinuous Galerkin (CDG) Method
   - Preconditioning for Newton-Krylov Solvers
   - Stabilization with Artificial Viscosity
3. Deformable Domains
   - Mapping-based ALE Formulation
   - Flapping Flight Applications
4. Large Deformation Solid Dynamics
   - High-Order Lagrangian DG Formulations
   - Applications: Thin structures, viscoplasticity
5. Conclusions

Jacobian Sparsity Structure

- Simple model of sparsity pattern: Connectivity of dual mesh, with large complete graphs $\boldsymbol{A}_{ij}$ in each cell
- Sizes of submatrices $\boldsymbol{A}_{ij}$ typically $>$ 100 DOFs
- Easy to obtain full BLAS performance! (e.g. in matvec or LU)

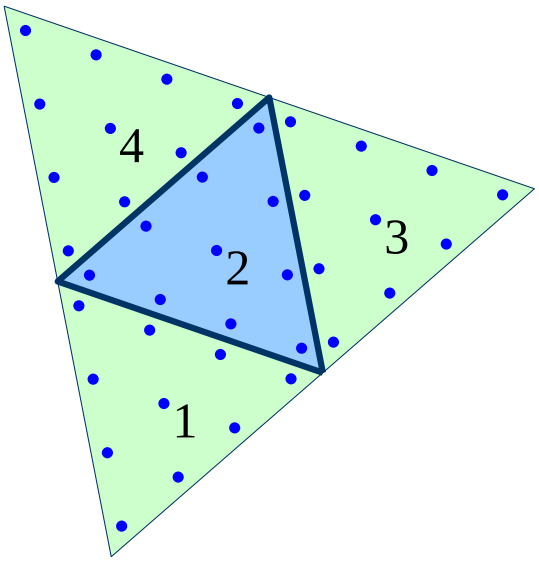

Block structure

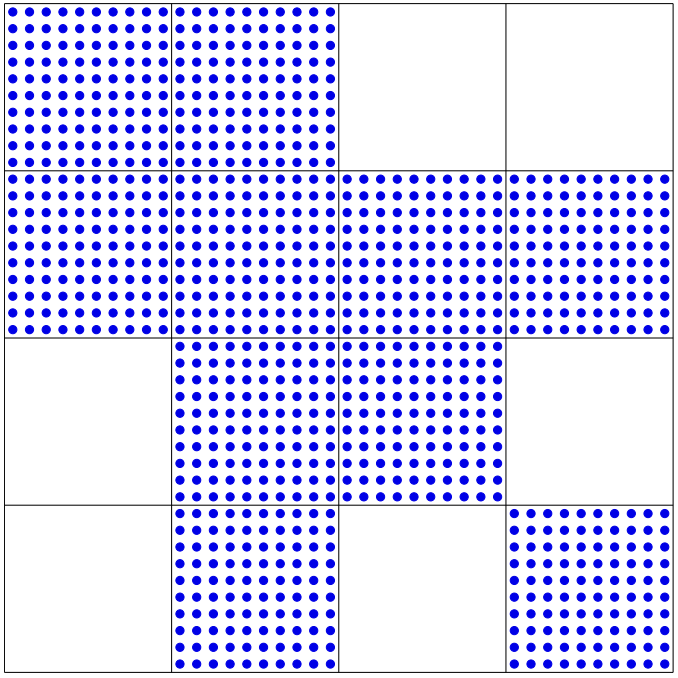

Preconditioners for Krylov Methods

- Preconditioning required for GMRES convergence
- Standard point-wise Jacobi, ILU, etc, ineffective for DG
- Some success with standard block-wise methods:
  - Block diagonal: $\boldsymbol{A} \approx \mathrm{blockdiag}(\boldsymbol{A})$
    - Poor in general
  - Block Incomplete LU: $\boldsymbol{A} \approx \tilde{\boldsymbol{L}}\tilde{\boldsymbol{U}}$
    - Good for convection (with the right ordering, more later)
  - p-multigrid (low-degree) preconditioner
    - Good for diffusion
- Highly efficient combination [Persson/Peraire 06]
  - Use block ILU(0) as post-smoother for coarse scale correction
  - Combines advantages of ILU and low-degree preconditioners
  - Cheap general purpose preconditioner

Minimum Discarded Fill Element Ordering

- Performance of ILU(0) highly dependent of ordering
- Greedy algorithm for element ordering [Persson/Peraire 07]:
  At step j, if j' is chosen next, we would discard the fill

$$\Delta\tilde{\boldsymbol{U}}_{ik}^{(j,j')} = -\tilde{\boldsymbol{U}}_{ij'}\tilde{\boldsymbol{U}}_{j'j'}^{-1}\tilde{\boldsymbol{U}}_{j'k}, \quad \text{for neighbors } i \geq j, k \geq j \text{ of element } j'$$

- Choose the j' that minimizes the norm of the discarded fill

$$w^{(j,j')} = \|\Delta\tilde{\boldsymbol{U}}^{(j,j')}\|_{\mathrm{F}}$$

- Some simplifications, min-heap data structure $\Longrightarrow \mathcal{O}(n \log n)$ cost
- Similar to the *Minimum Degree* algorithm, but considering the magnitude of the fill instead of just the size
- Related to the *Minimum Discarded Fill* algorithm [D'Azevedo, Forsyth, Tang 92]

The ILU(0)-p1 Preconditioner

- Combination of block ILU and multigrid [Persson/Peraire 06]
- Coarse scale correction + post-smoothing by $\tilde{\boldsymbol{A}} = \tilde{\boldsymbol{L}}\tilde{\boldsymbol{U}}$:

0. $\boldsymbol{A}^{(0)} = \boldsymbol{P}^T\boldsymbol{A}\boldsymbol{P}$	*Precompute coarse operator, block wise*
1. $\boldsymbol{b}^{(0)} = \boldsymbol{P}^T\boldsymbol{b}$	*Restrict residual element/component wise*
2. $\boldsymbol{A}^{(0)}\boldsymbol{u}^{(0)} = \boldsymbol{b}^{(0)}$	*Solve coarse scale problem*
3. $\boldsymbol{u} = \boldsymbol{P}\boldsymbol{u}^{(0)}$	*Prolongate solution element/component wise*
4. $\boldsymbol{u} = \boldsymbol{u} + \alpha\tilde{\boldsymbol{A}}^{-1}(\boldsymbol{b} - \boldsymbol{A}\boldsymbol{u})$	*Apply smoother $\tilde{\boldsymbol{A}}$ with damping α*

- Restriction/prolongation operator $\boldsymbol{P}$ block diagonal, based on orthogonal Koornwinder polynomials
- Coarse scale problem solved directly (2-D problems, serial) or iteratively by GMRES or h-multigrid

Effect of Ordering on Convection-Diffusion

- Convection-Diffusion model problem, with $(\alpha, \beta) = (1, 2x)$, $\varepsilon \geq 0$:

$$\frac{\partial u}{\partial t} + \nabla \cdot \begin{bmatrix} \alpha u \\ \beta u \end{bmatrix} - \nabla \cdot \begin{bmatrix} \varepsilon u_x \\ \varepsilon u_y \end{bmatrix} = 0$$

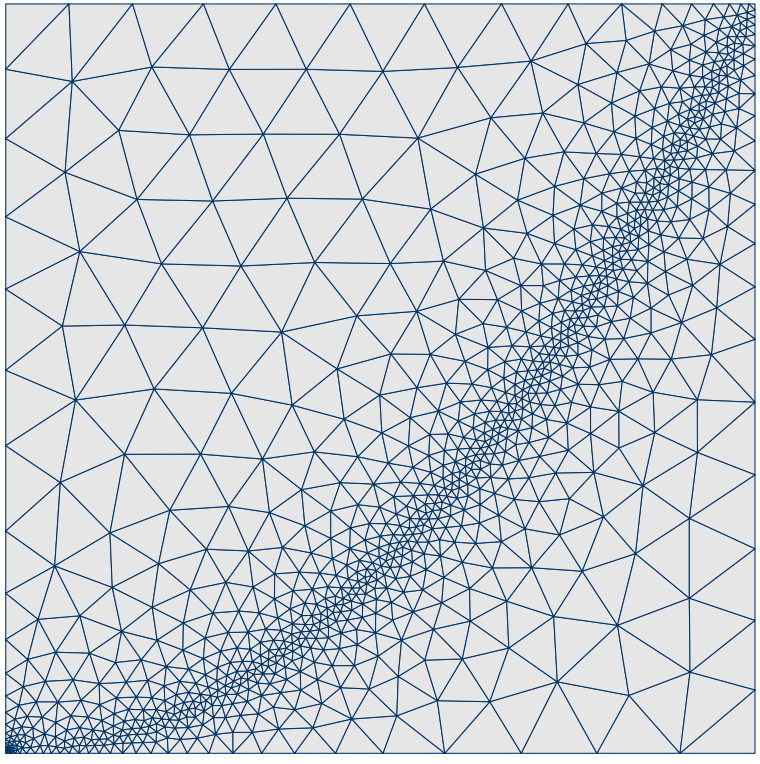

The ILU-p1 Preconditioner - Convection-Diffusion

- Block ILU perfect for convection, multigrid perfect for diffusion
- Block ILU-smoothed multigrid (BILU0-p1) almost perfect for any ε

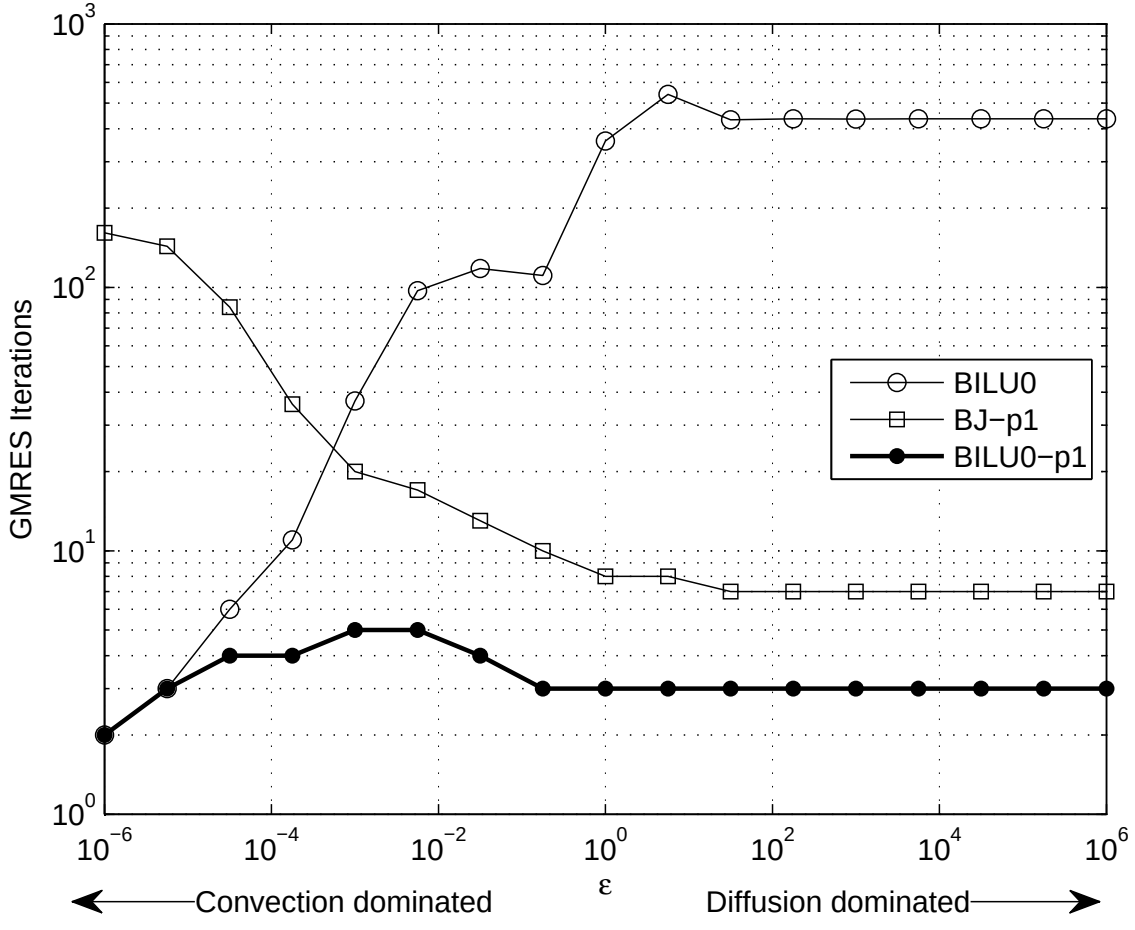

The ILU-p1 Preconditioner – Navier-Stokes

- Model Navier-Stokes problem for wide range of Reynolds numbers

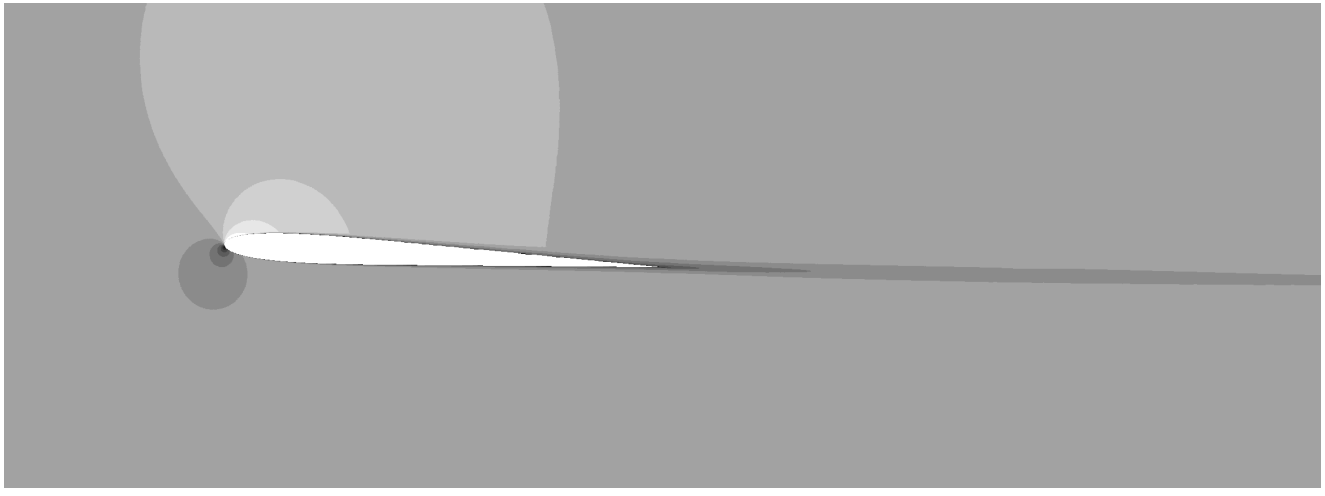

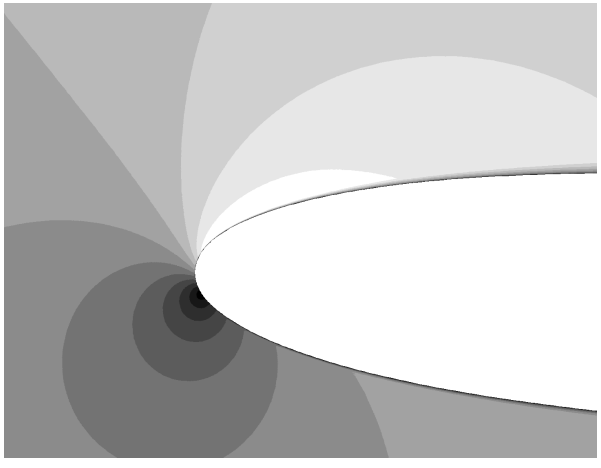

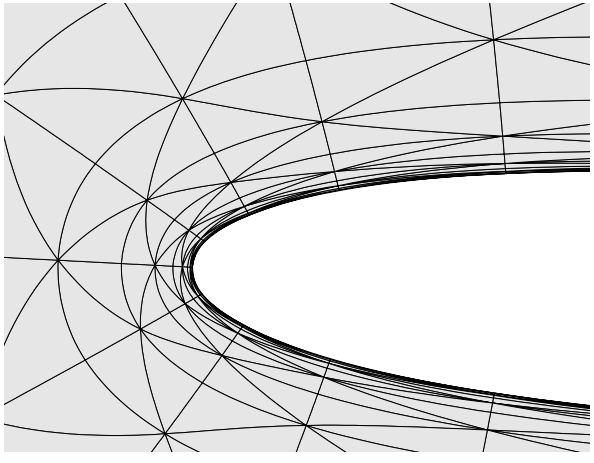

The ILU-p1 Preconditioner – Navier-Stokes

- Convergence for various Reynolds numbers, Δt, and M
- $\times$= No convergence after 1,000 iterations

Problem	Parameters		Preconditioner/Iterations		
	Δt	M	Block Jacobi-p1	Block GS-p1	Block ILU0-p1
Inviscid	10^{-3}	0.2	19	11	4
	10^{-1}	0.2	85	49	6
	∞	0.2	142	72	9
	10^{-3}	0.01	112	67	6
	10^{-1}	0.01	$\times$	532	10
	∞	0.01	$\times$	$\times$	16
Laminar	10^{-3}	0.2	34	19	4
Re=1,000	10^{-1}	0.2	597	225	5
	∞	0.2	$\times$	$\times$	7
	10^{-3}	0.01	66	33	5
	10^{-1}	0.01	619	207	9
	∞	0.01	$\times$	748	12

The ILU-p1 Preconditioner – Navier-Stokes

- Convergence for various Reynolds numbers, Δt, and M
- $\times$ = No convergence after 1,000 iterations

Problem	Parameters		Preconditioner/Iterations		
	Δt	M	Block Jacobi-p1	Block GS-p1	Block ILU0-p1
Laminar	10^{-3}	0.2	19	11	4
Re=20,000	10^{-1}	0.2	220	113	8
	∞	0.2	$\times$	$\times$	20
	10^{-3}	0.01	90	38	6
	10^{-1}	0.01	$\times$	735	16
	∞	0.01	$\times$	$\times$	35
RANS	10^{-3}	0.2	56	28	7
Re=10^6	10^{-1}	0.2	$\times$	$\times$	25
	∞	0.2	$\times$	$\times$	18
	10^{-3}	0.01	231	110	9
	10^{-1}	0.01	$\times$	$\times$	16
	∞	0.01	$\times$	$\times$	28

Mach Number Dependence

- Excellent convergence for Mach number $M << 1$ with BILU0-p1

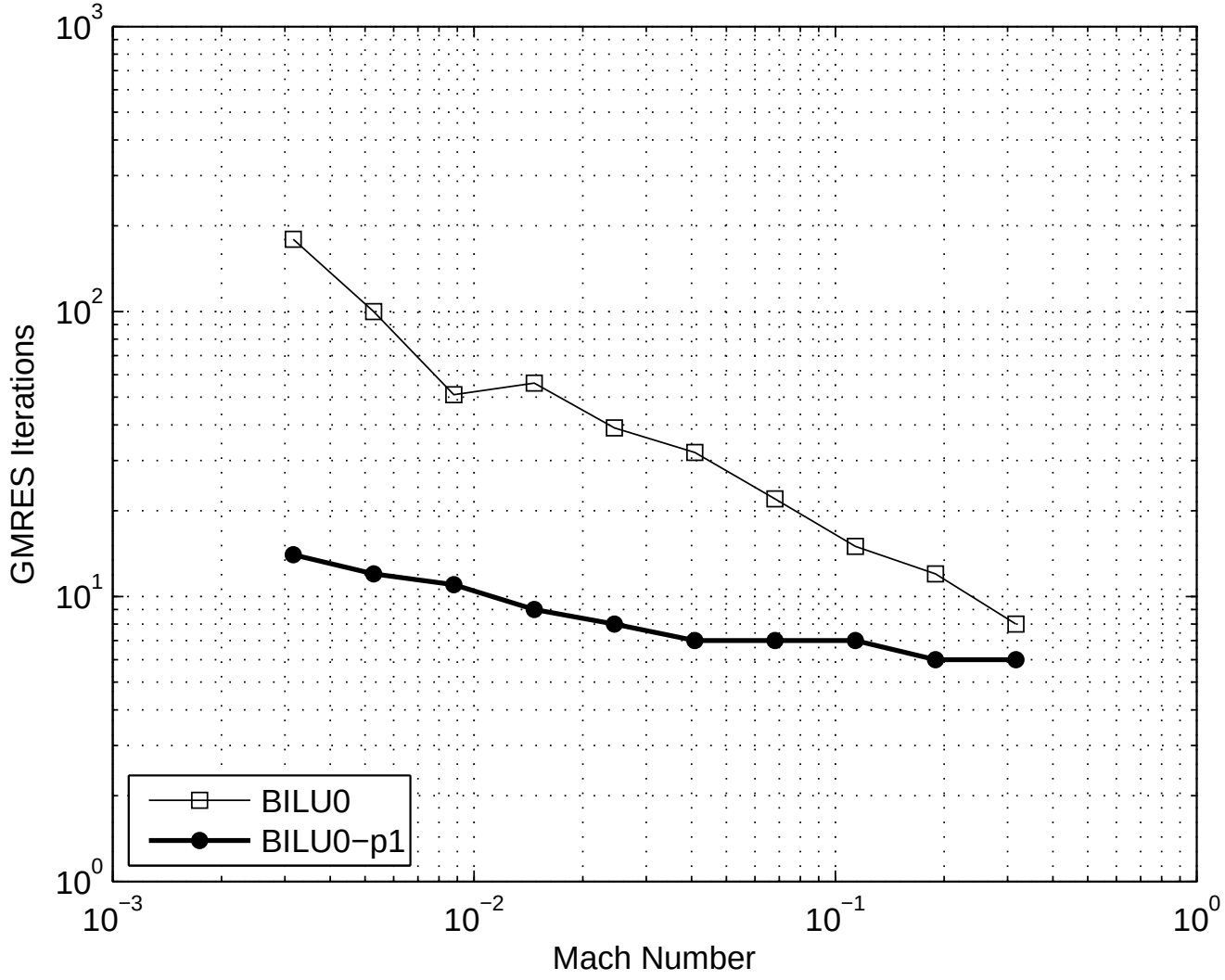

Outline

1. Introduction
2. Discretization and Solvers
   - High-Order Mesh Generation
   - The Discontinuous Galerkin Method
   - The Compact Discontinuous Galerkin (CDG) Method
   - Preconditioning for Newton-Krylov Solvers
   - Stabilization with Artificial Viscosity
3. Deformable Domains
   - Mapping-based ALE Formulation
   - Flapping Flight Applications
4. Large Deformation Solid Dynamics
   - High-Order Lagrangian DG Formulations
   - Applications: Thin structures, viscoplasticity
5. Conclusions

Artificial Viscosity for Underresolved Features

- Cannot resolve all solution features (shocks, RANS, singularities)
- Low dissipation makes DG sensitive to underresolution
- Detect by sensors and add viscosity [Persson/Peraire 06,07]
- Enables shock capturing with sub-cell resolution and robust solution of Spalart-Alamaras RANS model

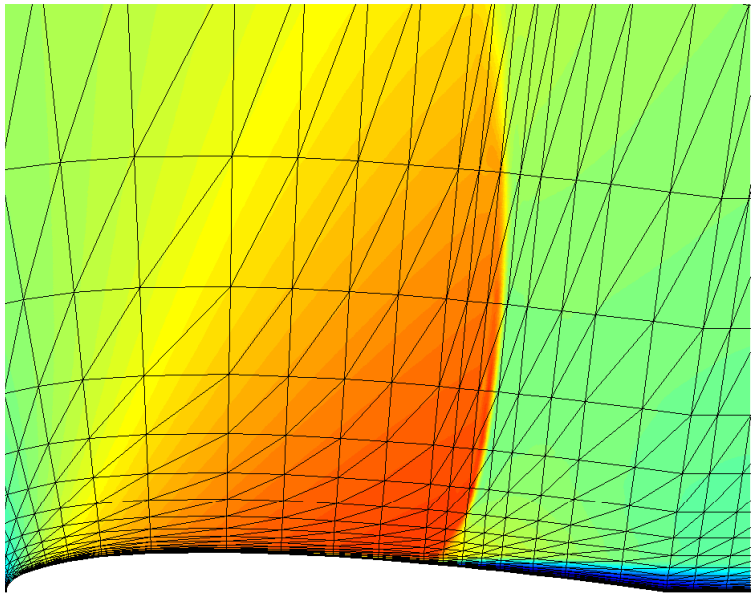

Mach

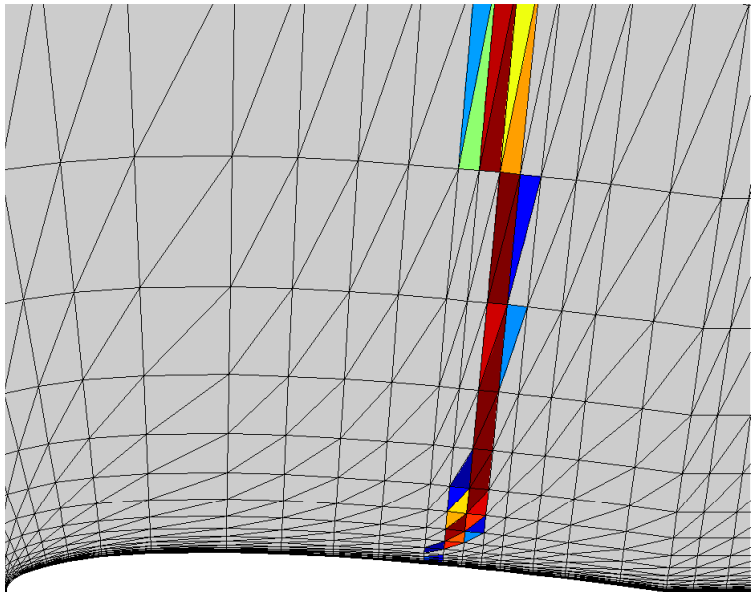

Sensor

Shock Sensor

- Regularity of solution determined from the decay rate of expansion coefficients in orthogonal basis
- Example: Periodic Fourier case: $f(x) = \sum_{k=-\infty}^{\infty} g_k e^{ikx}$
  If $f(x)$ has m continuous derivatives $\rightarrow$ $|g_k| \sim k^{-(m+1)}$
- For simplices: Expand solution in orthonormal Koornwinder basis:

$$u = \sum_{i=1}^{N(p)} u_i \psi_i, \quad \hat{u} = \sum_{i=1}^{N(p-1)} u_i \psi_i, \quad s_e = \log_{10}\left(\frac{(u-\hat{u}, u-\hat{u})_e}{(u,u)_e}\right)$$

- Determine elemental piecewise constant ε_e

$$\varepsilon_e = \begin{cases} 0 & \text{if} \quad s_e < s_0 - \kappa \\ \frac{\varepsilon_0}{2}\left(1 + \sin\frac{\pi(s_e - s_0)}{2\kappa}\right) & \text{if} \quad s_0 - \kappa \le s_e \le s_0 + \kappa \\ \varepsilon_0 & \text{if} \quad s_e > s_0 + \kappa \end{cases} .$$

where $\varepsilon_0 \sim h/p$, $s_0 \sim 1/p^4$ and κ empirical

Euler Equations – Artificial Viscosity Models

- Laplacian: $\frac{\partial \boldsymbol{u}}{\partial t} + \nabla \cdot \mathcal{F}(\boldsymbol{u}) = \nabla \cdot (\epsilon \nabla \boldsymbol{u})$
- Physical: $\frac{\partial \boldsymbol{u}}{\partial t} + \nabla \cdot \mathcal{F}(\boldsymbol{u}) = \nabla \cdot \mathcal{F}_v(\boldsymbol{u}; \mathrm{Re}, \mathrm{Pr})$

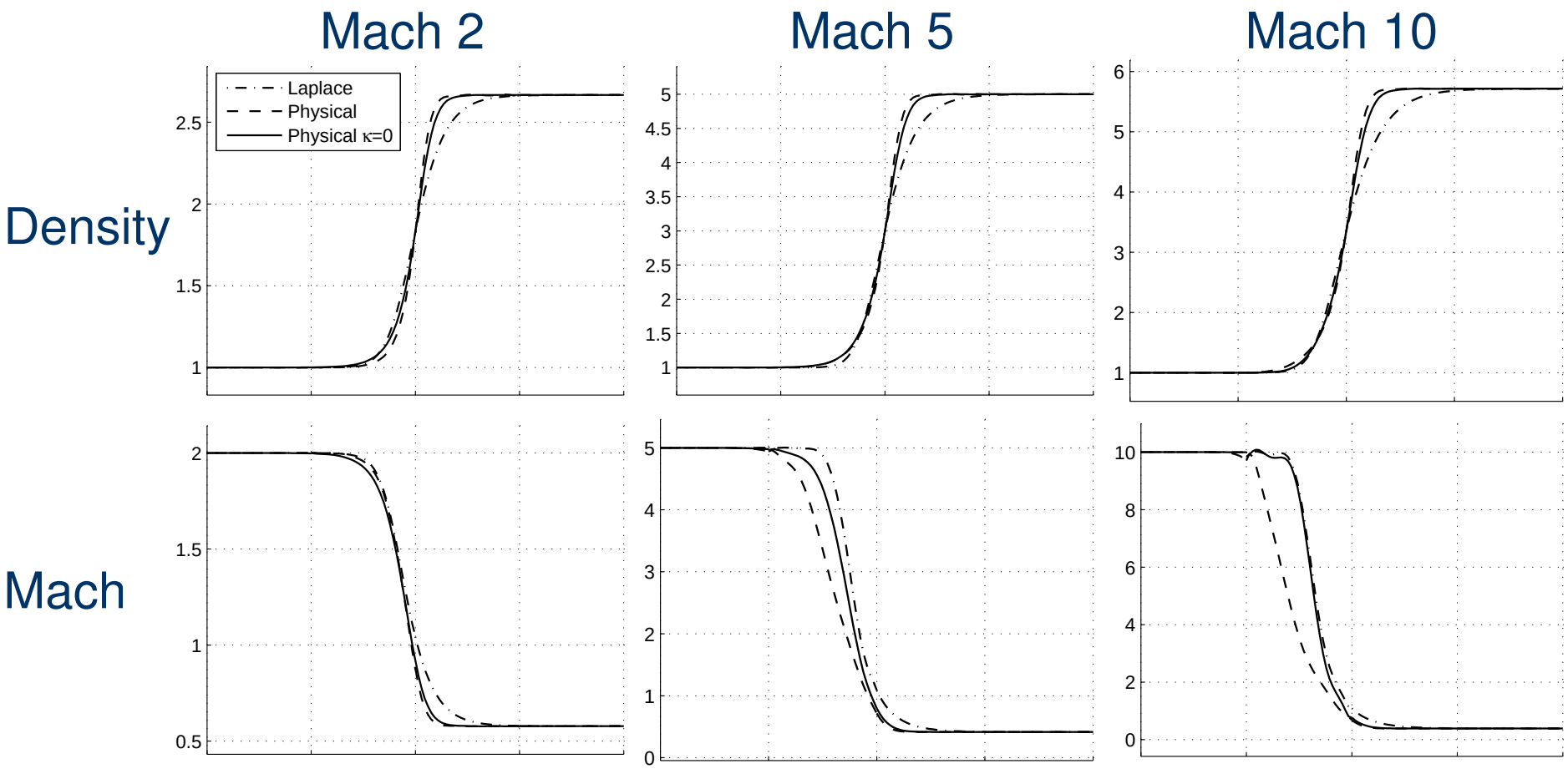

Example: RAE2822

- Turbulent RANS flow ($M = 0.675, \alpha = 2.31^o, \mathrm{Re} = 6.5 \cdot 10^6$)
- p-converged solution, fixed resolution h/p

$p = 2$ (constant h/p) $p = 4$

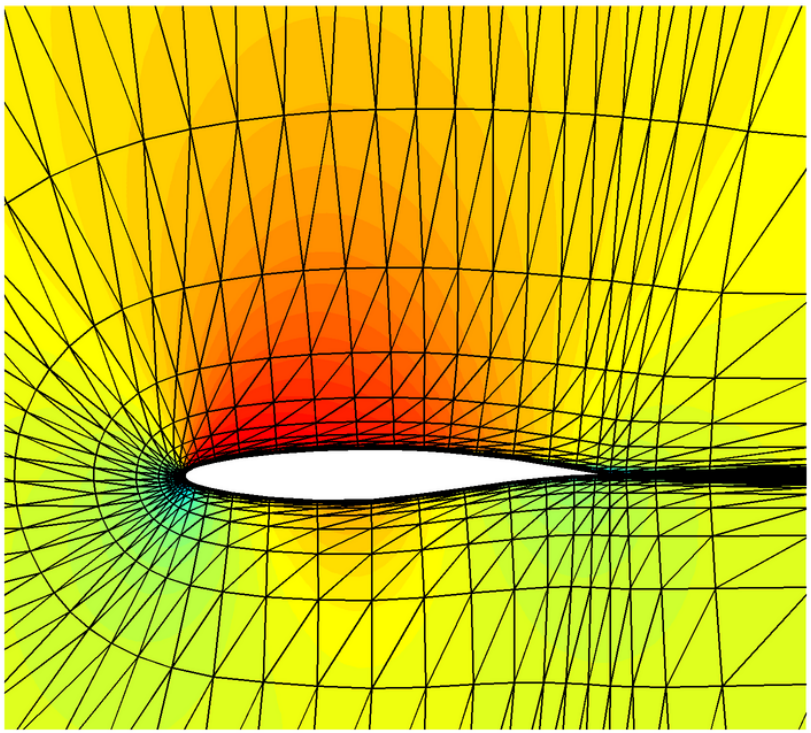

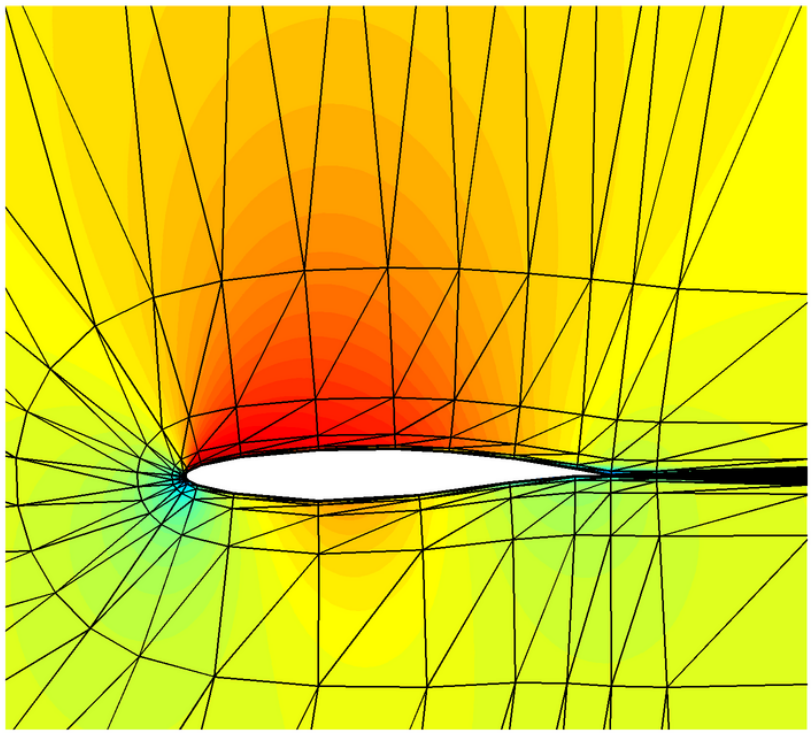

$C_L = 0.6144 \quad C_D = 0.0104$

$C_L = 0.6131 \quad C_D = 0.0103$

Example: RAE2822

- Turbulent RANS flow ($M = 0.675, \alpha = 2.31^o, \mathrm{Re} = 6.5 \cdot 10^6$)
- p-converged solution, fixed resolution h/p

$p = 2$ (constant h/p) $p = 4$

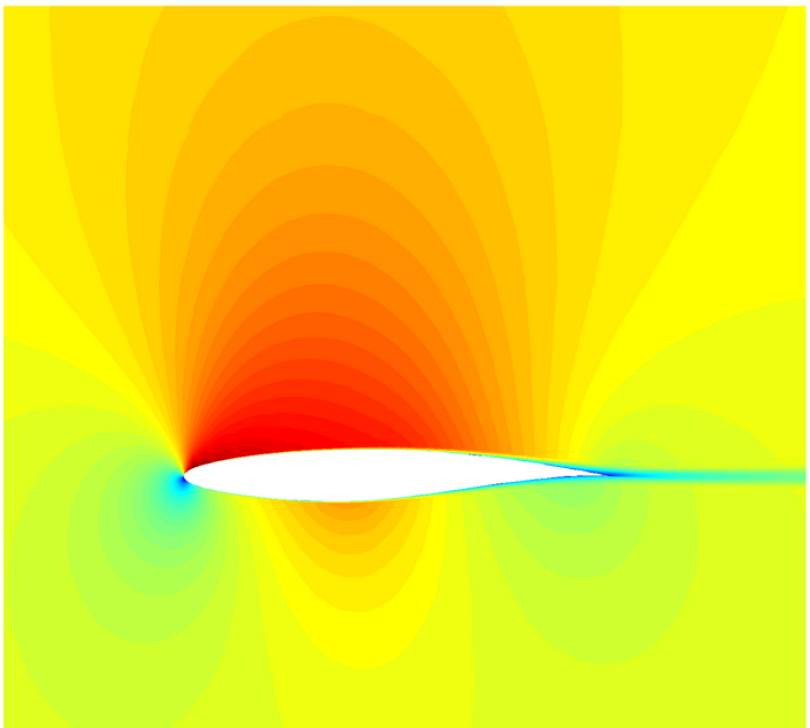

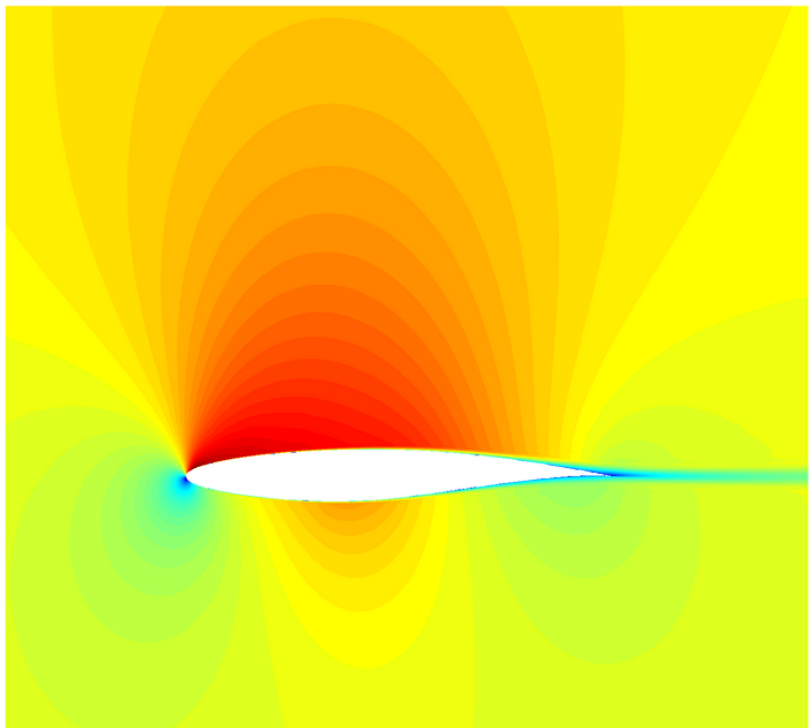

$C_L = 0.6144 \quad C_D = 0.0104$

$C_L = 0.6131 \quad C_D = 0.0103$

Example: RAE2822

- Highly accurate boundary forces even with coarse meshes

C_p

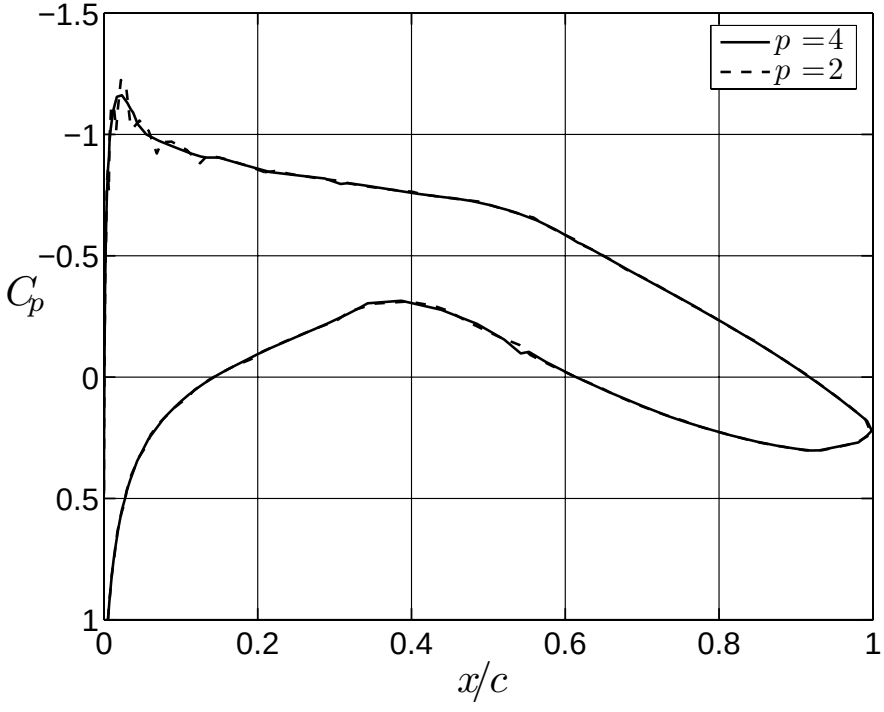

C_f

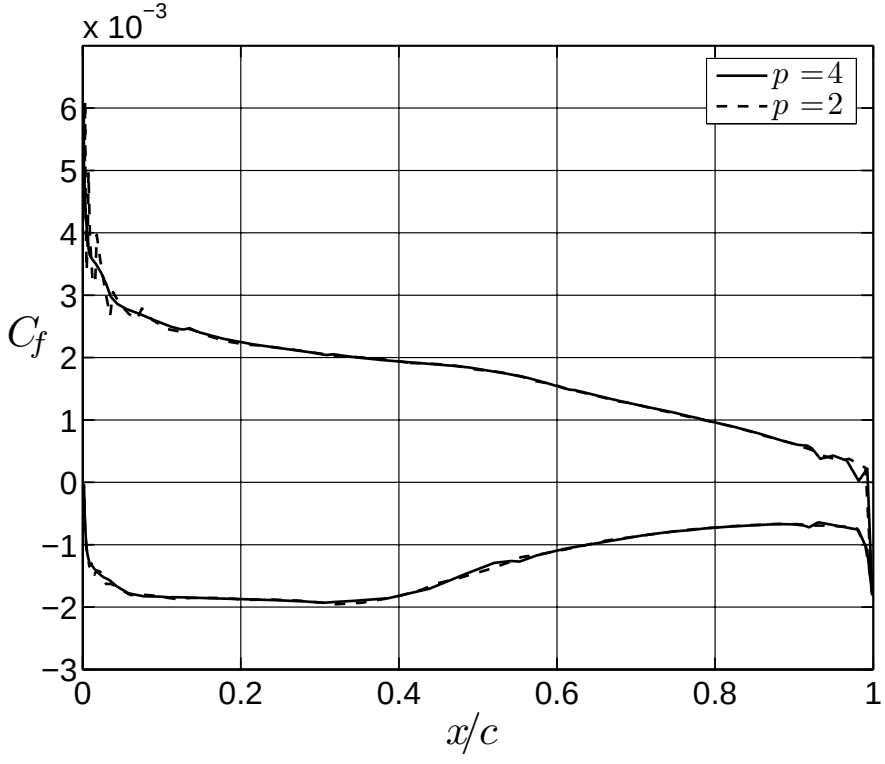

Example: RAE2822, Transonic

- Transonic flow ($M = 0.729, \mathrm{Re} = 6.5 \cdot 10^6$)
- Sub-cell resolution of shocks

$p = 4$

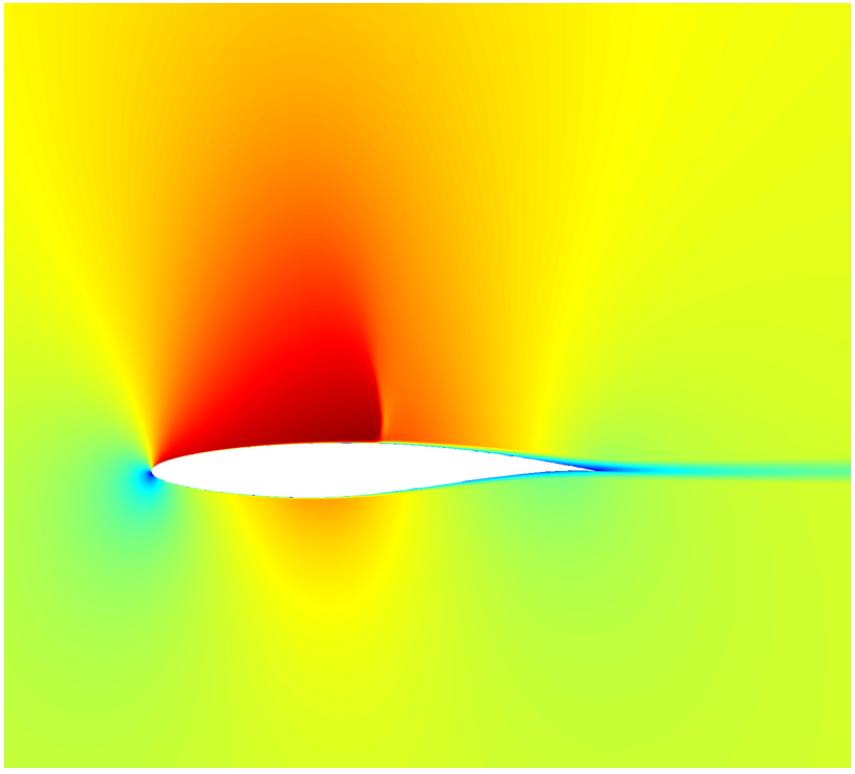

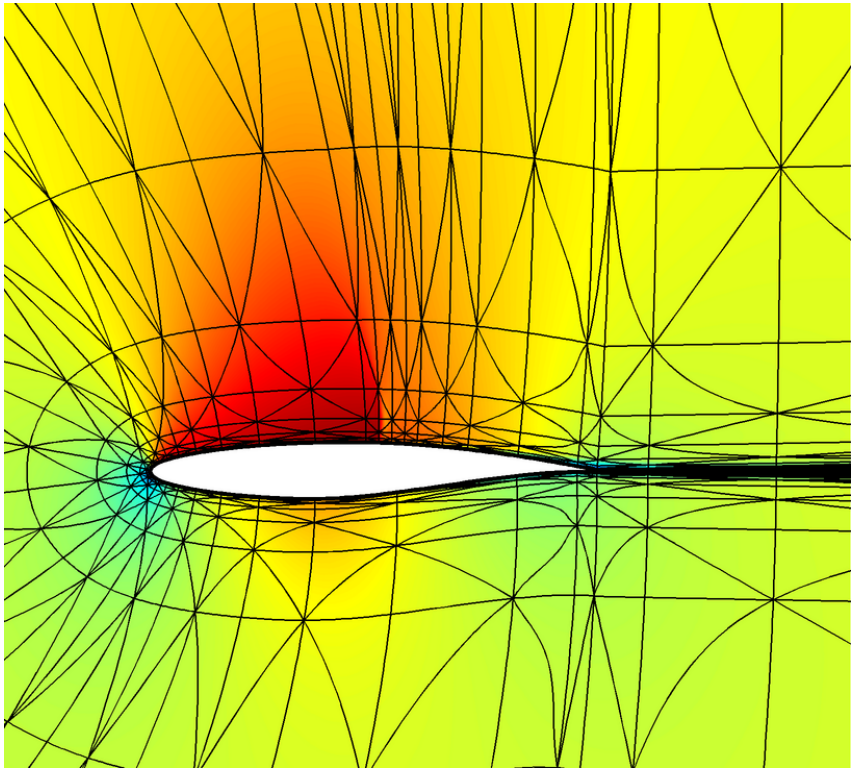

Example: RAE2822, Transonic

- Transonic flow ($M = 0.729, \mathrm{Re} = 6.5 \cdot 10^6$)
- Sub-cell resolution of shocks

$p = 4$

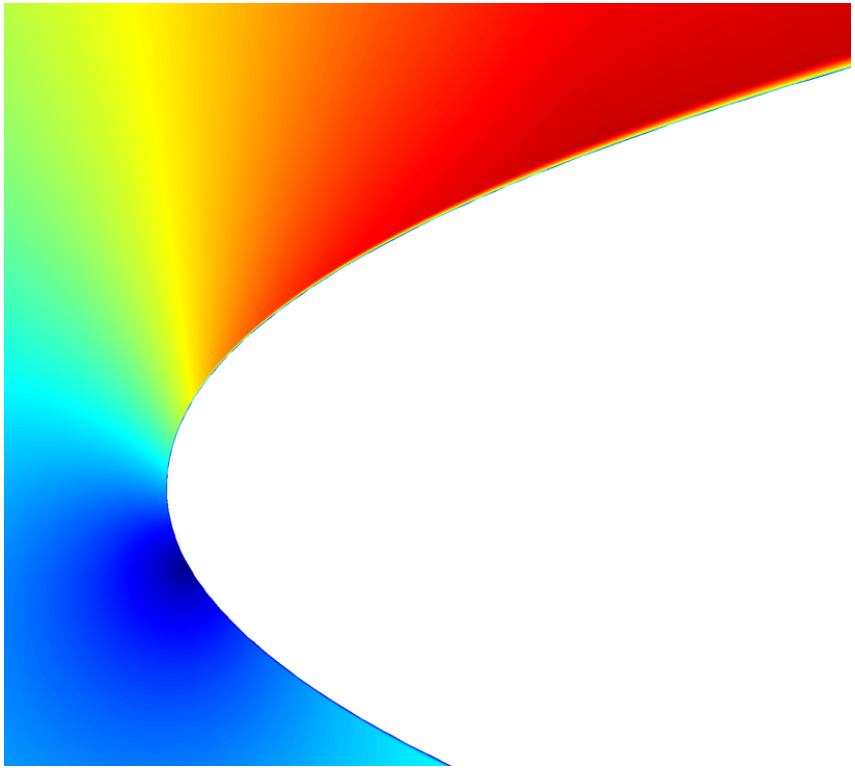

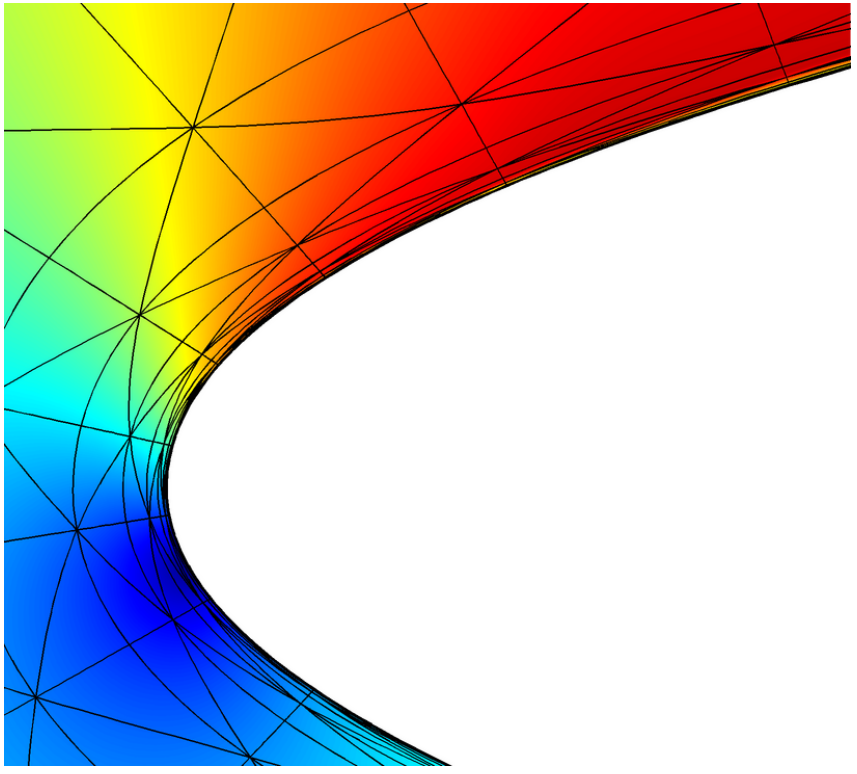

Outline

1. Introduction
2. Discretization and Solvers
   - High-Order Mesh Generation
   - The Discontinuous Galerkin Method
   - The Compact Discontinuous Galerkin (CDG) Method
   - Preconditioning for Newton-Krylov Solvers
   - Stabilization with Artificial Viscosity
3. Deformable Domains
   - Mapping-based ALE Formulation
   - Flapping Flight Applications
4. Large Deformation Solid Dynamics
   - High-Order Lagrangian DG Formulations
   - Applications: Thin structures, viscoplasticity
5. Conclusions

Methods for Deforming Domains

- Many ALE formulations for unstructured meshes
  - Equations discretized on a deforming grid, time-dependent metric
  - At most third order accuracy in space and time demonstrated
- Alternative approach for finite differences [Visbal/Gaitonde 02]
  - Map from fixed reference domain to time-varying physical domain
  - Correction for the Geometric Conservation Law (GCL) with sources
- Our method: Mapping approach in a DG setting, with a conservative formulation for satisfying the GCL
  - Guaranteed stability
  - Arbitrary orders of accuracy in space and time

ALE Formulation

- Map from reference domain V to physical deformable domain $v(t)$
- A point $\boldsymbol{X}$ in V is mapped to a point $\boldsymbol{x}(t) = \boldsymbol{G}(\boldsymbol{X}, t)$ in $v(t)$
- Introduce the *mapping deformation gradient* $\boldsymbol{G}$ and the *mapping velocity* $\boldsymbol{v}_X$ as

$$\boldsymbol{G} = \nabla_X \boldsymbol{G}$$

$$\boldsymbol{v}_X = \left.\frac{\partial \boldsymbol{G}}{\partial t}\right|_X$$

and set $g = \det(\boldsymbol{G})$

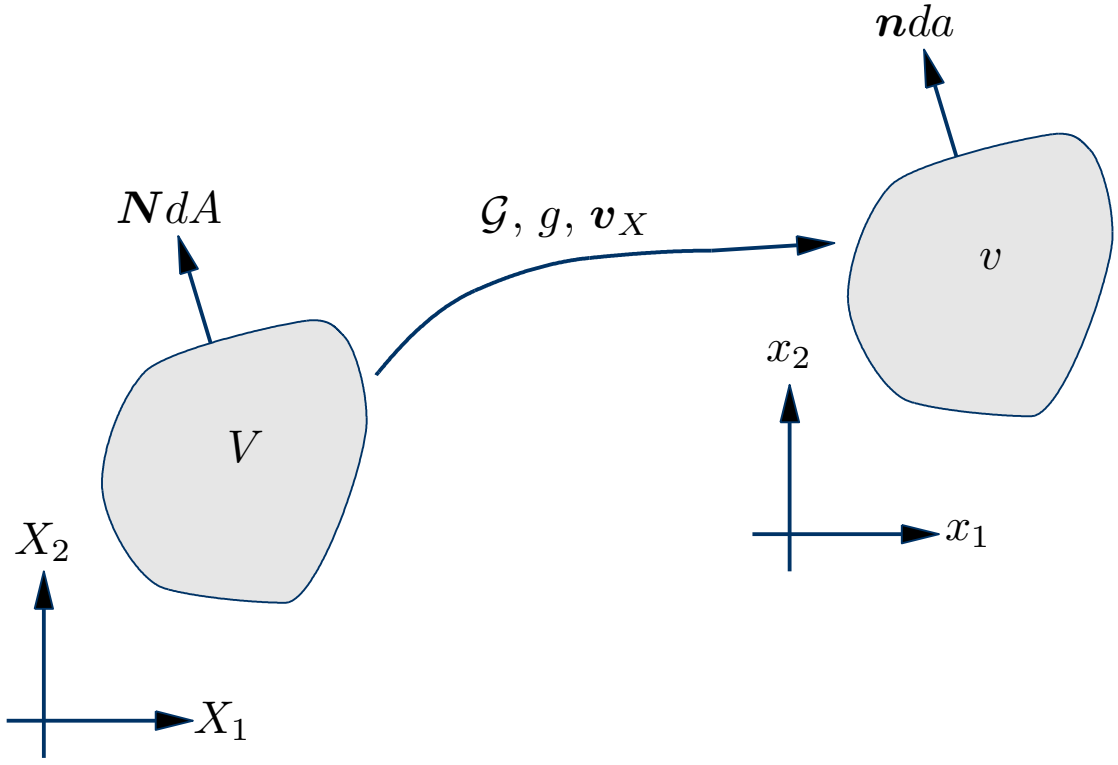

Transformed Equations

- The system of conservation laws in the physical domain $v(t)$

$$\left.\frac{\partial \boldsymbol{U}_x}{\partial t}\right|_x + \boldsymbol{\nabla}_x \cdot \boldsymbol{F}_x(\boldsymbol{U}_x, \boldsymbol{\nabla}_x \boldsymbol{U}_x) = 0$$

  can be written in the reference configuration V as

$$\left.\frac{\partial \boldsymbol{U}_X}{\partial t}\right|_X + \boldsymbol{\nabla}_X \cdot \boldsymbol{F}_X(\boldsymbol{U}_X, \boldsymbol{\nabla}_X \boldsymbol{U}_X) = 0$$

  where

$$\boldsymbol{U}_X = g\boldsymbol{U}_x \,, \qquad \boldsymbol{F}_X = g\boldsymbol{G}^{-1}\boldsymbol{F}_x - \boldsymbol{U}_X\boldsymbol{G}^{-1}\boldsymbol{v}_X$$

  and

$$\boldsymbol{\nabla}_x \boldsymbol{U}_x = \boldsymbol{\nabla}_X(g^{-1}\boldsymbol{U}_X)\boldsymbol{G}^{-T} = (g^{-1}\boldsymbol{\nabla}_X \boldsymbol{U}_X - \boldsymbol{U}_X \boldsymbol{\nabla}_X(g^{-1}))\boldsymbol{G}^{-T}$$

- *Proof.* See [Persson/Peraire/Bonet 07]

Geometric Conservation Law

- A constant solution in $v(t)$ is not necessarily a solution in V, due to inexact integration of the Jacobian g
  - The time evolution of g is

$$\left.\frac{\partial g}{\partial t}\right|_X - \boldsymbol{\nabla}_X \cdot (g\boldsymbol{G}^{-1}\boldsymbol{v}_X) = 0 \ ,$$

    which in general is non-zero
- Visbal and Gaitonde added source terms to cancel the errors
- Our approach solves instead the conservative system

$$\left.\frac{\partial(\bar{g}g^{-1}\boldsymbol{U}_X)}{\partial t}\right|_X - \boldsymbol{\nabla}_X \cdot \boldsymbol{F}_X = \boldsymbol{0}$$

$$\left.\frac{\partial \bar{g}}{\partial t}\right|_X - \boldsymbol{\nabla}_X \cdot (g\boldsymbol{G}^{-1}\boldsymbol{v}_X) = 0$$

Example: Euler Vortex

- Propagate an Euler vortex on a variable domain with

$$x(\xi,\eta,t) = \xi + 2.0\sin(2\pi\xi/20)\sin(\pi\eta/7.5)\sin(1.0\cdot 2\pi t/t_0)$$
$$y(\xi,\eta,t) = \eta + 1.5\sin(2\pi\xi/20)\sin(\pi\eta/7.5)\sin(2.0\cdot 2\pi t/t_0)$$

- Mapped scheme – Everything is computed on the reference mesh

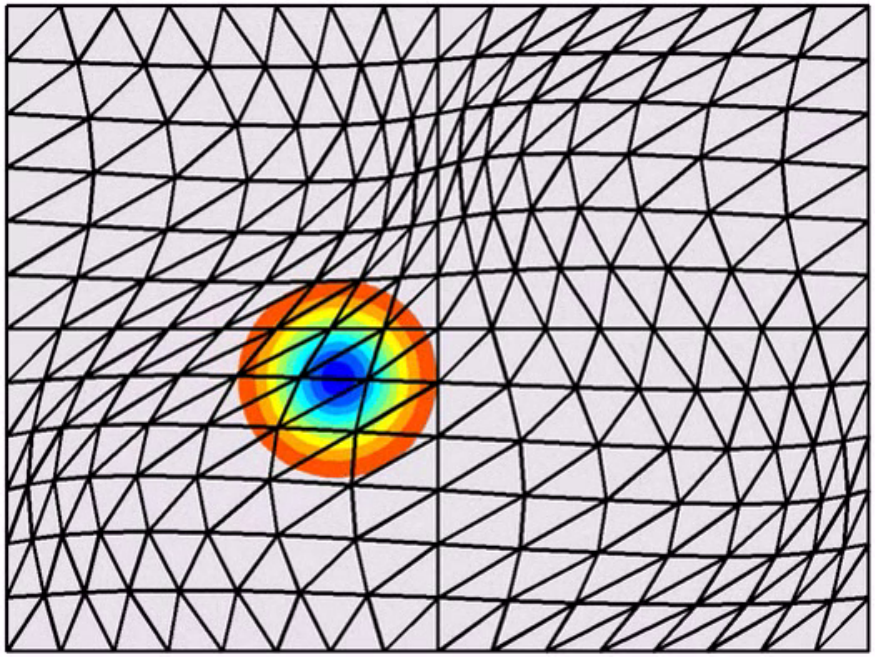

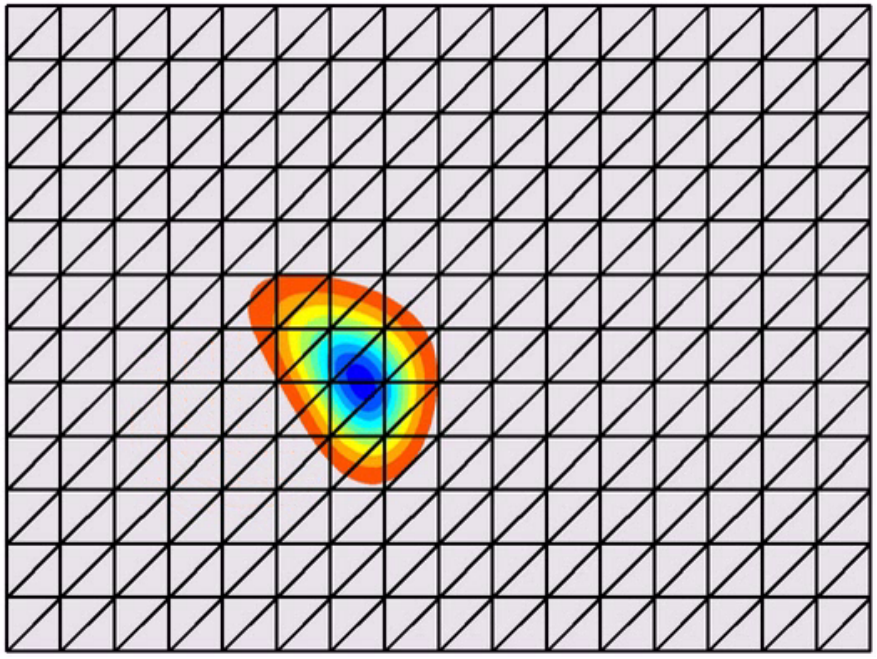

Example: Euler Vortex, Convergence

- Optimal order of convergence $O(h^{p+1})$ for mapped scheme

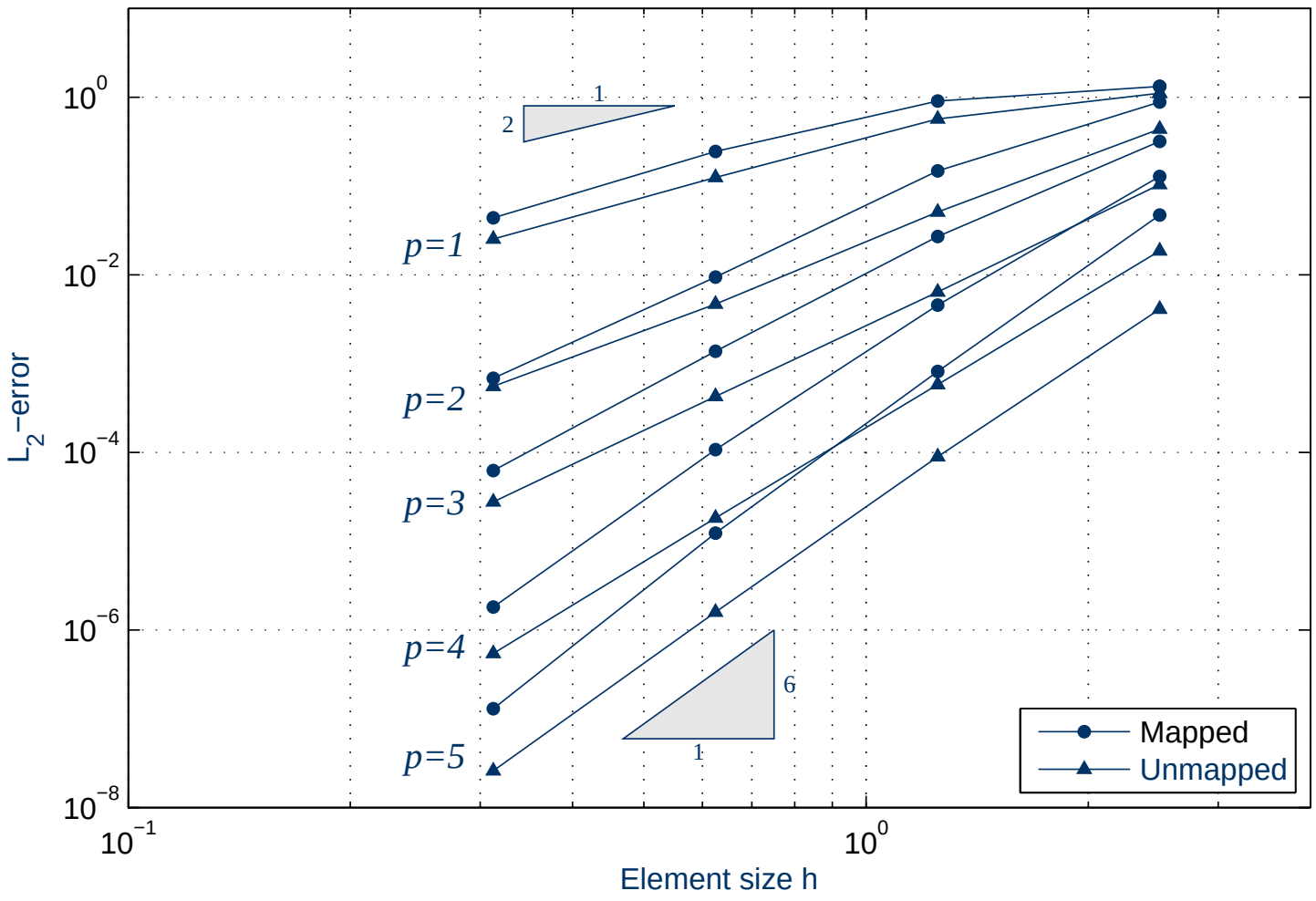

Outline

1. Introduction
2. Discretization and Solvers
   - High-Order Mesh Generation
   - The Discontinuous Galerkin Method
   - The Compact Discontinuous Galerkin (CDG) Method
   - Preconditioning for Newton-Krylov Solvers
   - Stabilization with Artificial Viscosity
3. Deformable Domains
   - Mapping-based ALE Formulation
   - Flapping Flight Applications
4. Large Deformation Solid Dynamics
   - High-Order Lagrangian DG Formulations
   - Applications: Thin structures, viscoplasticity
5. Conclusions

Biologically-Inspired Flapping Flight

- Development of computational tools for studying flapping flight
- Challenging problems: Deforming domains, fluid-structure interaction, transitional flows, etc

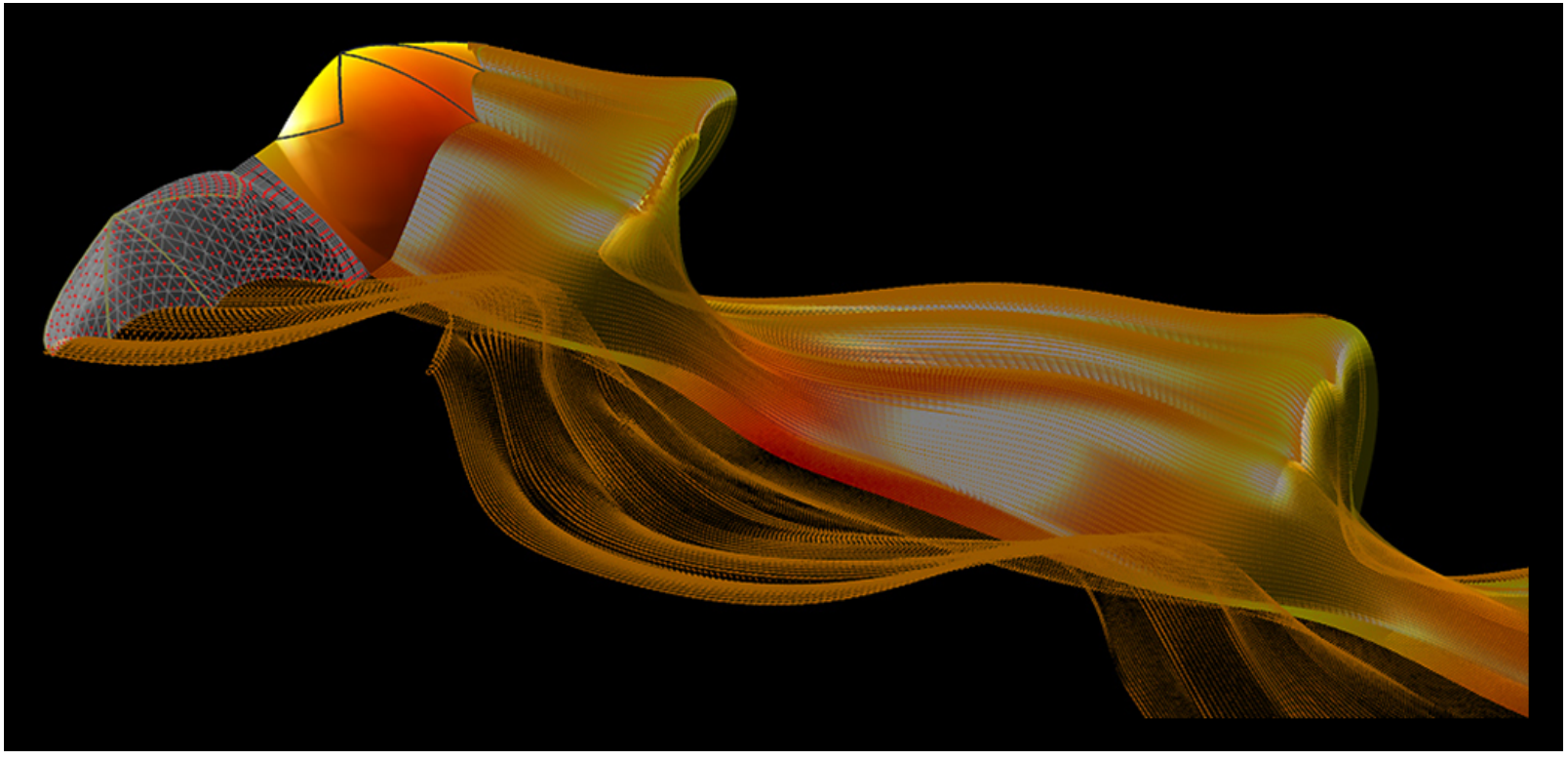

Example: Pitching Airfoil

- Airfoil attached to translating and heaving point by torsional spring
- Fluid properties: $\mathrm{Re} = 5000$, $M = 0.2$
- Forced vertical motion $r_z(t) = r_0 \sin \omega t$ (at leading edge)
- Moment equation: $I\ddot{\theta} + C\theta - S\ddot{r}_z(t) + M_{\text{aero}} = 0$
  - I moment of inertia, C spring stiffness, $S = mx_c$ static unbalance
  - M_{aero} moment from fluid

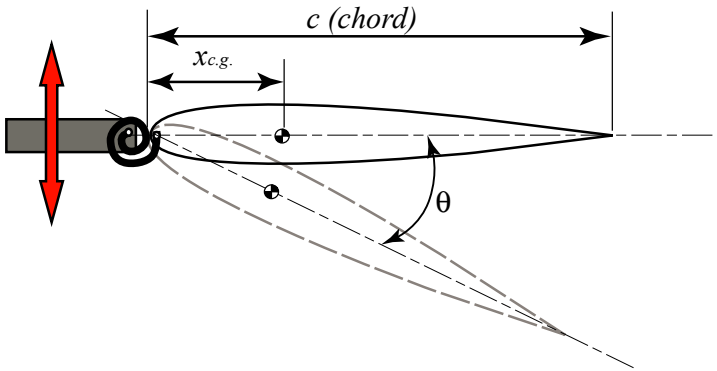

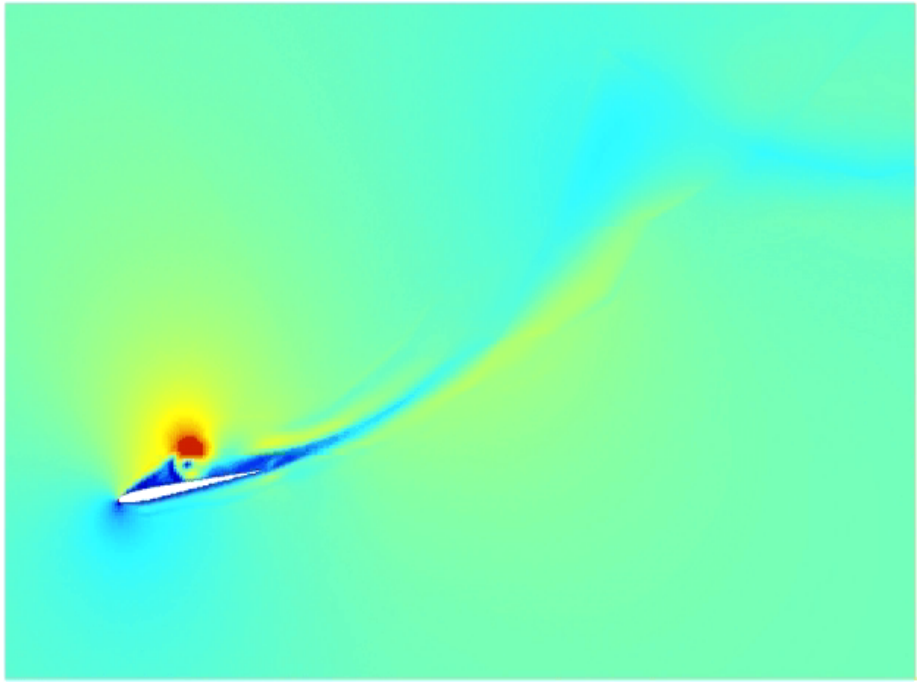

Example: Pitching Airfoil/Flapper Design

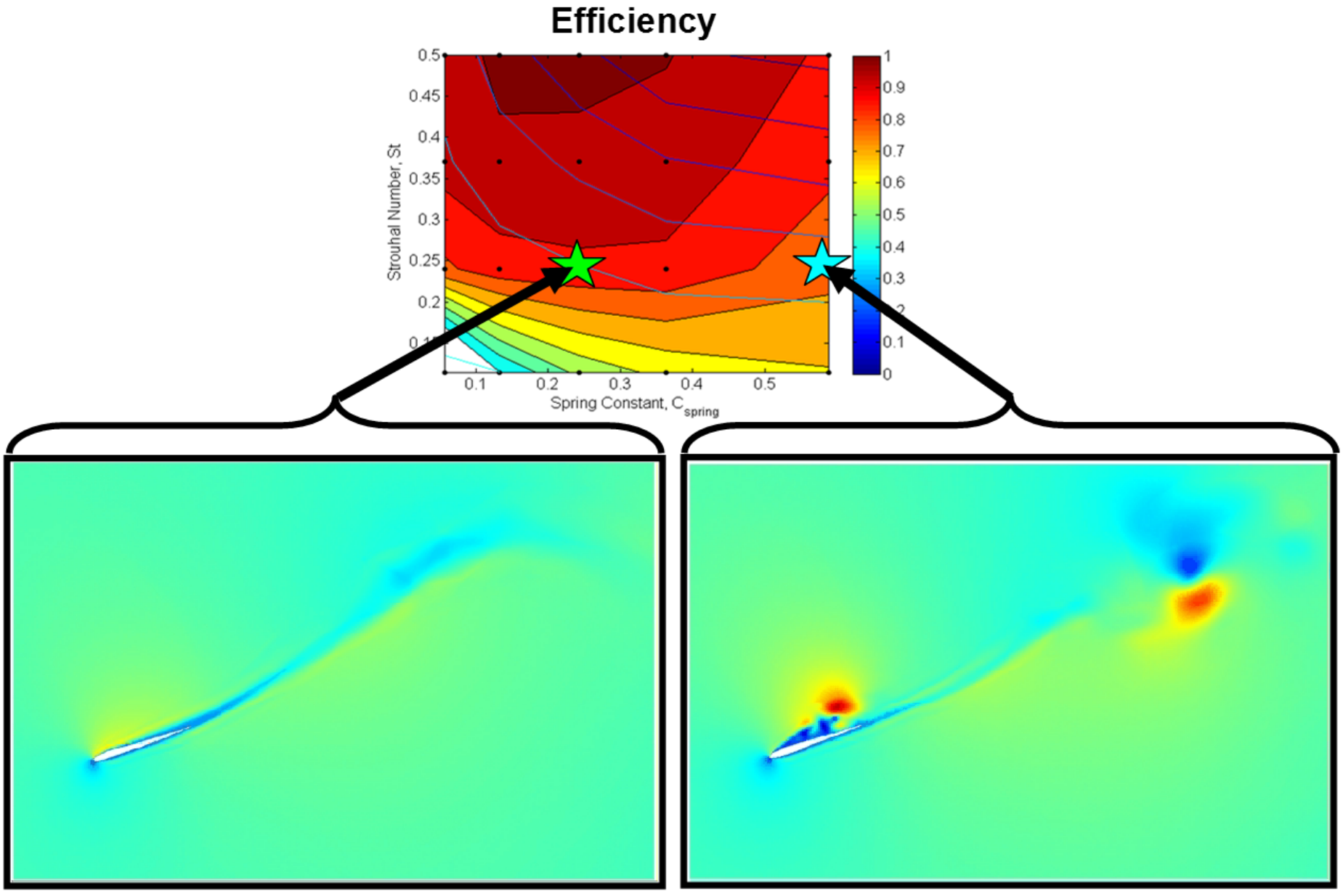

Example: Heaving and Pitching Foil in Wake

- NACA 0012 foil heaving and pitching in wake of D-section cylinder
- Both oscillate $y(t) = A\sin(2\pi ft)$, foil pitching $\theta = a\sin(2\pi ft + \pi/2)$
- Based on experimental study [Gopalkrishnan et al 94]

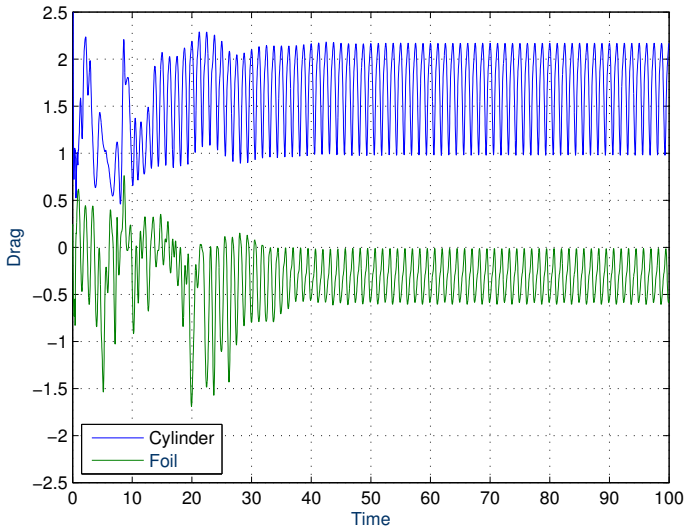

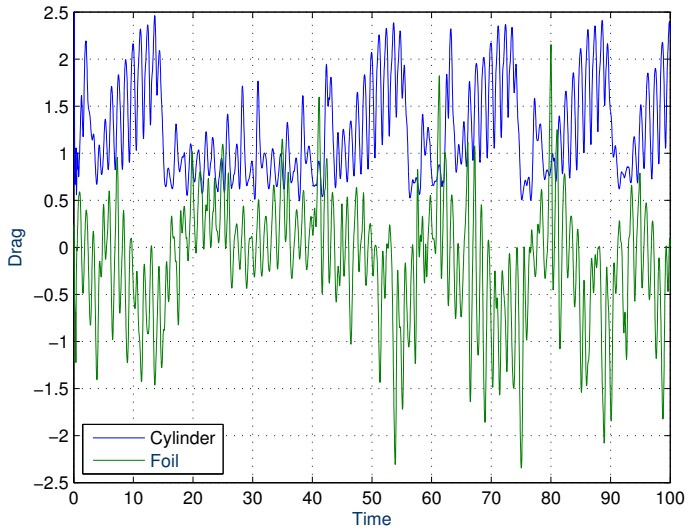

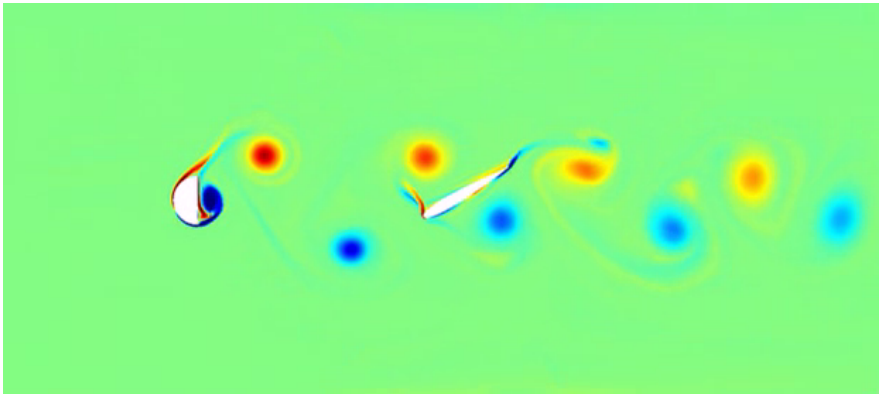

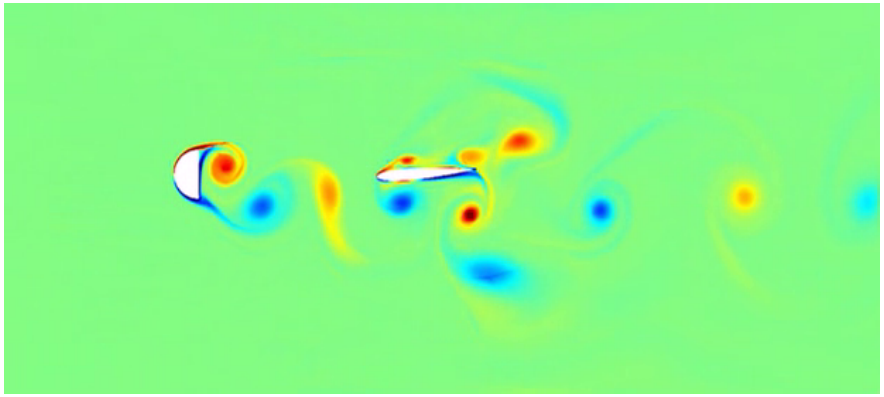

Example: Locomotion of Free Flapping Body

- Oscillating plate, unconstrained horizontally [Vandenberghe et al 04, Alben/Shelley 05]
- Instability breaks symmetry and forces plate into motion

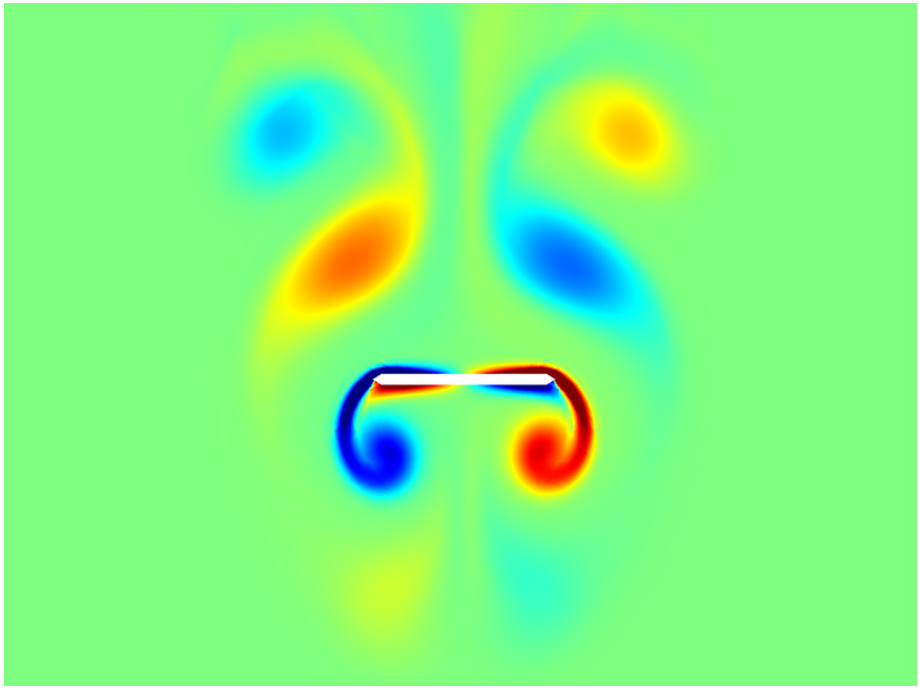

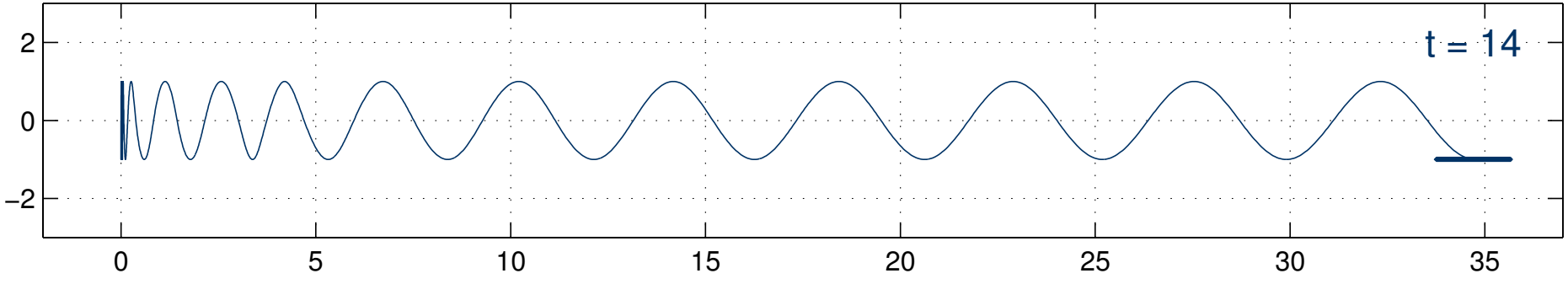

Example: Fluid-Structure Interaction

- Interaction between fluid and a hyperelastic membrane
- Compliancy can alleviate leading edge separation

Experiment (A. Song, Brown U)

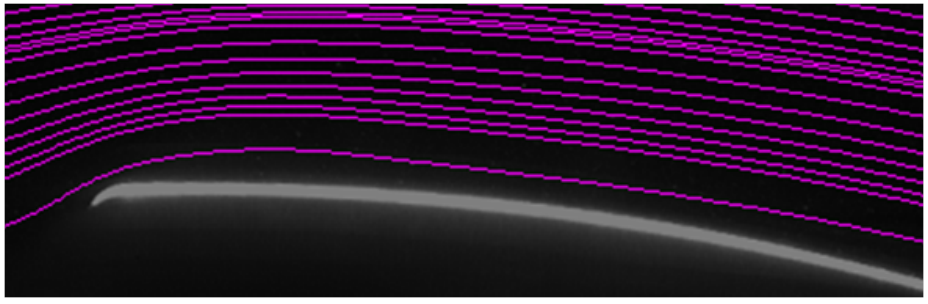

Compliant membrane

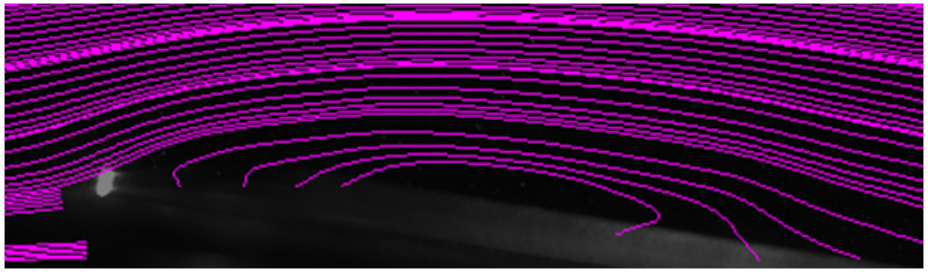

Rigid flat plate

Fluid/membrane simulation

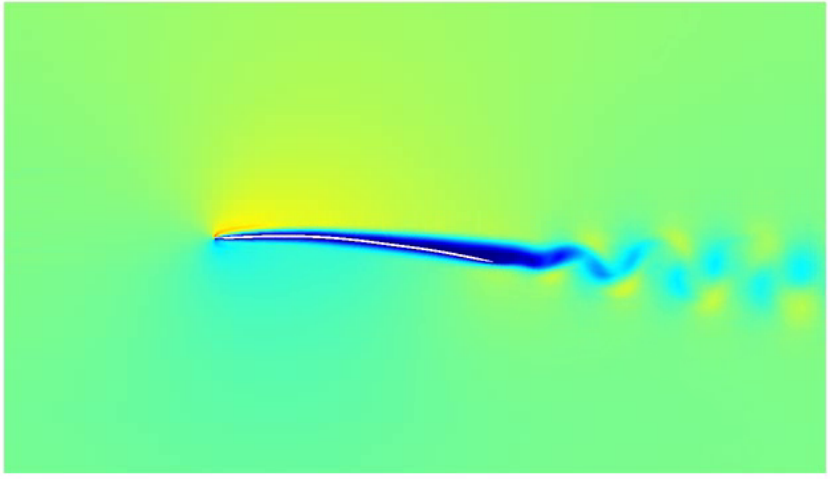

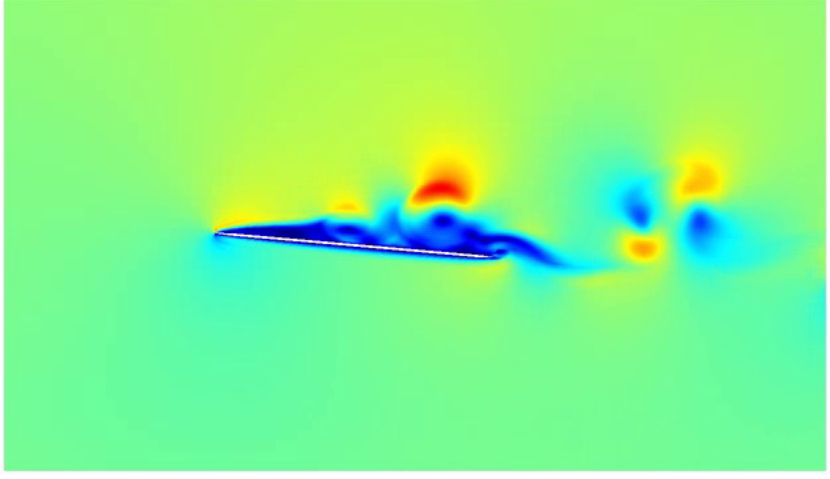

Example: Dragonfly, Compliant Wings

Experiment (A. Song, Brown U)

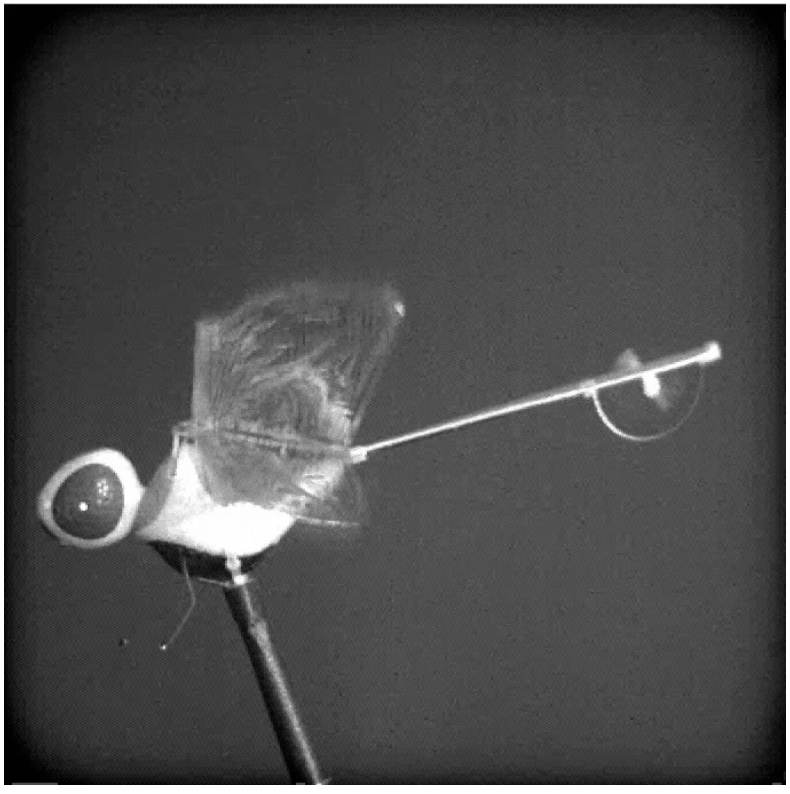

Fluid/membrane simulation

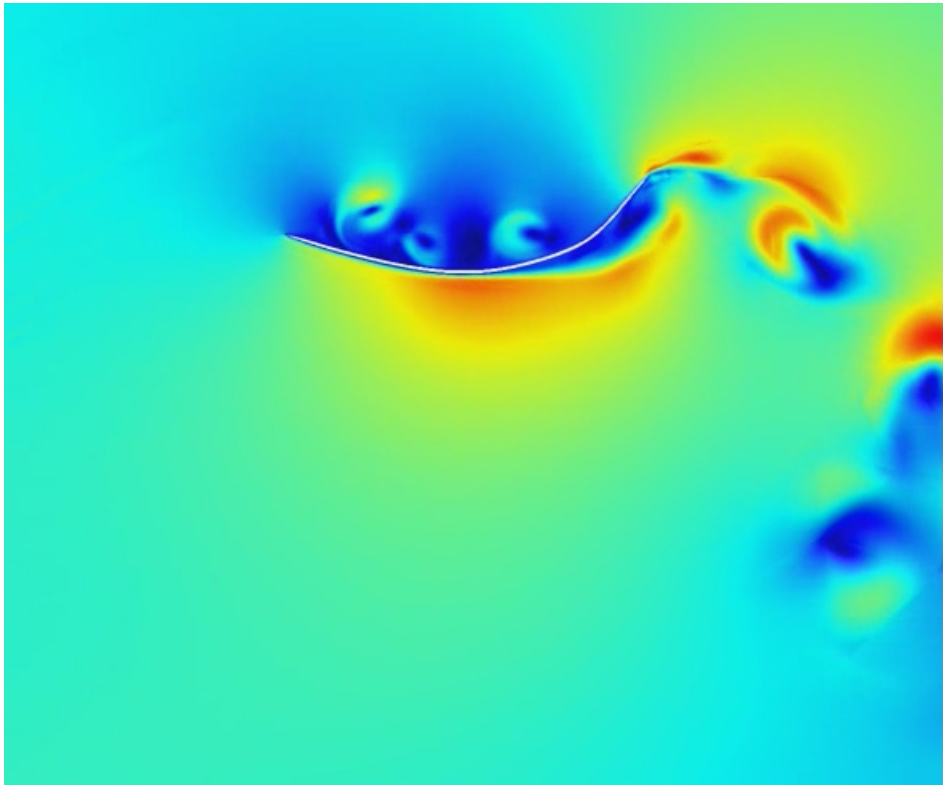

Outline

1. Introduction
2. Discretization and Solvers
   - High-Order Mesh Generation
   - The Discontinuous Galerkin Method
   - The Compact Discontinuous Galerkin (CDG) Method
   - Preconditioning for Newton-Krylov Solvers
   - Stabilization with Artificial Viscosity
3. Deformable Domains
   - Mapping-based ALE Formulation
   - Flapping Flight Applications
4. Large Deformation Solid Dynamics
   - High-Order Lagrangian DG Formulations
   - Applications: Thin structures, viscoplasticity
5. Conclusions

Lagrangian DG Formulation for Solid Dynamics

- Many potential benefits with DG for solid dynamics
- Arbitrary orders of accuracy with tetrahedral elements
- Discontinuous approach highly insensitive to locking

  $\Longrightarrow$ Almost incompressible materials

  $\Longrightarrow$ Thin structures (beams, shells) with highly stretched elements
- Stabilization for convection

  $\Longrightarrow$ High-order accurate ALE
- Block-diagonal mass matrix

  $\Longrightarrow$ Efficient explicit methods

Lagrangian Formulation

- Map from reference domain V to physical domain $v(t)$

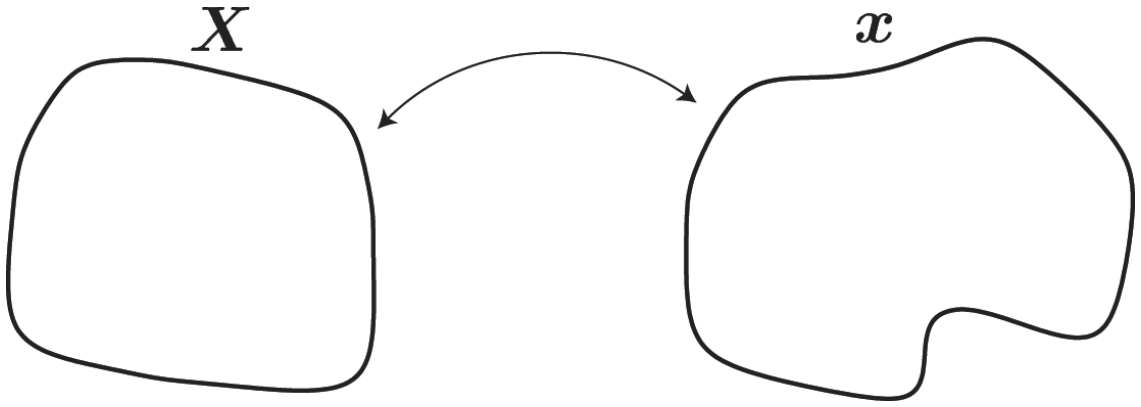

$$\boldsymbol{F} = \frac{\partial \boldsymbol{x}}{\partial \boldsymbol{X}} \,, \qquad J = \det \boldsymbol{F} \,, \qquad \boldsymbol{v}(\boldsymbol{X}, t) = \frac{\partial \boldsymbol{x}}{\partial t} \,, \qquad \boldsymbol{p} = \rho_0 \boldsymbol{v}$$

- Conservation of linear momentum:

$$\frac{d}{dt} \int_V \boldsymbol{p} \, dV = \int_V \rho_0 \boldsymbol{b} \, dV + \int_{\partial V} \boldsymbol{t} \, dA \,, \qquad \boldsymbol{t} = \boldsymbol{P}\boldsymbol{N}$$

$$\frac{\partial \boldsymbol{p}}{\partial t} = \boldsymbol{\nabla} \cdot \boldsymbol{P} + \rho_0 \boldsymbol{b}$$

with *first Piola-Kirchhoff stress tensor* $\boldsymbol{P}(\boldsymbol{F})$

Hyperelastic Neo-Hookean Constitutive Model

- Strain Energy Potential

$$\psi(\boldsymbol{F}) = \psi_{iso}(J^{-1/3}\boldsymbol{F}) + \psi_{vol}(J)$$

$$\psi_{iso} = \frac{\mu}{2}[tr(J^{-2/3}\boldsymbol{F} : \boldsymbol{F}) - 3] \ , \qquad \psi_{vol} = \frac{1}{2}\kappa(J-1)^2$$

- First Piola-Kirchhoff Stress Tensor

$$\boldsymbol{P} = \boldsymbol{P}_{dev} + \boldsymbol{P}_{vol} \ ; \ \boldsymbol{P}_{dev} = \frac{\partial \psi_{iso}}{\partial \boldsymbol{F}} \ , \ \boldsymbol{P}_{vol} = \frac{\partial \psi_{vol}}{\partial \boldsymbol{F}}$$

$$\boldsymbol{P}_{vol} = \frac{d\psi_{vol}(J)}{dJ}\frac{\partial J}{\partial \boldsymbol{F}} = pJ\boldsymbol{F}^{-T} \ ; \ p = \frac{d\psi_{vol}(J)}{dJ} = \kappa(J-1)$$

$$\boldsymbol{P}_{dev} = \mu J^{-2/3}[\boldsymbol{F} - \frac{1}{3}(\boldsymbol{F} : \boldsymbol{F})\boldsymbol{F}^{-T}]$$

Second-Order Formulation

- Straight-forward second-order formulation in terms of material points $\boldsymbol{x}$ and momentum $\boldsymbol{p}$:

$$\frac{\partial \boldsymbol{x}}{\partial t} = \boldsymbol{p}/\rho_0$$
$$\frac{\partial \boldsymbol{p}}{\partial t} - \nabla \cdot \boldsymbol{P}(\boldsymbol{F}) = \rho_0 \boldsymbol{b}$$

- Computationally inexpensive, first equation essentially an ODE
- Full pth order polynomial spaces for $\boldsymbol{x}$ and $\boldsymbol{p}$
- Use CDG scheme for stable discretization of second derivatives
- However, conservative treatment of shocks unclear

First-Order Conservation Law Formulation

- Solve for momentum $\boldsymbol{p}$ and deformation gradient $\boldsymbol{F}$
- Time evolution of the deformation gradient:

$$\frac{\partial \boldsymbol{F}}{\partial t} = \boldsymbol{\nabla}(\boldsymbol{p}/\rho_0) \qquad \text{or} \qquad \frac{\partial \boldsymbol{F}}{\partial t} = \boldsymbol{\nabla} \cdot \left(\frac{1}{\rho_0} \boldsymbol{p} \otimes \boldsymbol{I} \right)$$

- Write as system of conservation laws:

$$\mathcal{U}_t + \nabla \cdot \mathcal{F}(\mathcal{U}) = \mathcal{S}(\mathcal{U})$$

with

$$\mathcal{U} = \begin{pmatrix} \boldsymbol{p} \\ \boldsymbol{F} \end{pmatrix}, \quad \mathcal{F} = \begin{pmatrix} \boldsymbol{P} \\ \frac{1}{\rho_0} \boldsymbol{p} \otimes \boldsymbol{I} \end{pmatrix}, \quad \mathcal{S} = \begin{pmatrix} \rho_0 \boldsymbol{b} \\ \boldsymbol{0} \end{pmatrix}$$

- Conservative formulation $\Longrightarrow$ borrow shock capturing from CFD, jump conditions physically meaningful
- However, computationally expensive, needs curl-free spaces for $\boldsymbol{F}$

Oscillating Beam, Energy Conservation

- Energy conservation not explicitly enforced by scheme
- Therefore, it is a good indicator of accuracy

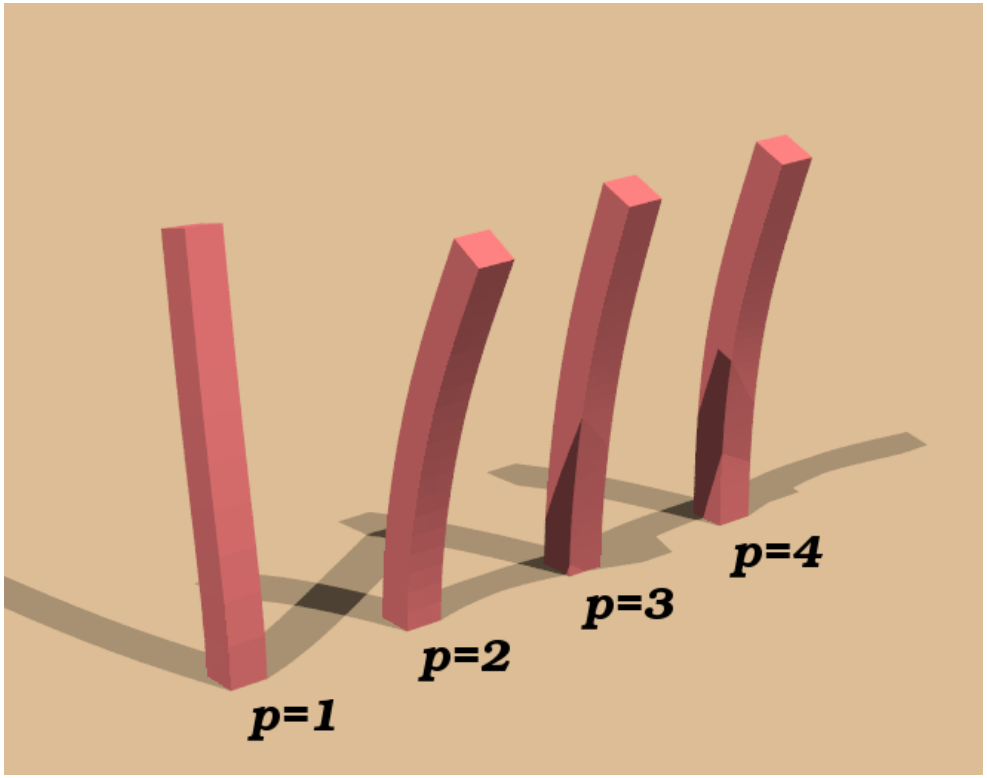

Kinetic, potential, and total energy

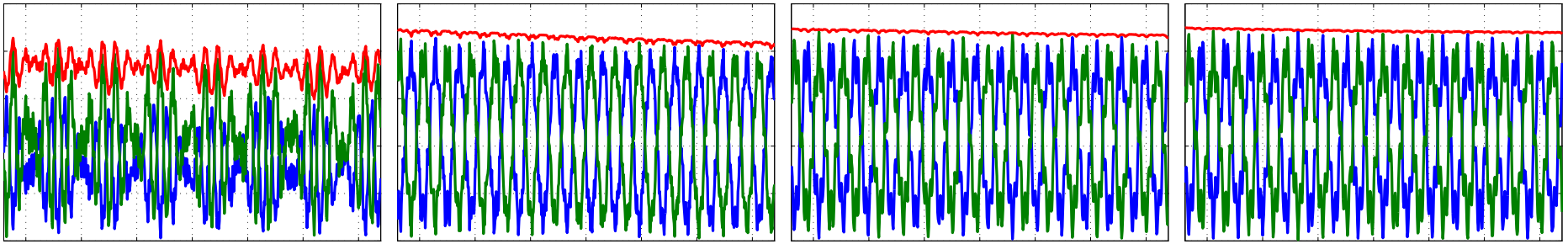

$p = 1$ $p = 2$ $p = 3$ $p = 4$

Outline

1. Introduction
2. Discretization and Solvers
   - High-Order Mesh Generation
   - The Discontinuous Galerkin Method
   - The Compact Discontinuous Galerkin (CDG) Method
   - Preconditioning for Newton-Krylov Solvers
   - Stabilization with Artificial Viscosity
3. Deformable Domains
   - Mapping-based ALE Formulation
   - Flapping Flight Applications
4. Large Deformation Solid Dynamics
   - High-Order Lagrangian DG Formulations
   - Applications: Thin structures, viscoplasticity
5. Conclusions

Volumetric Modeling of Thin Structures

- The high order elements allow for high stretching
- Discontinuous basis functions highly insensitive to locking
- Model plate problem: Uniform loading, small deformations
- High order convergence rates for $p > 1$

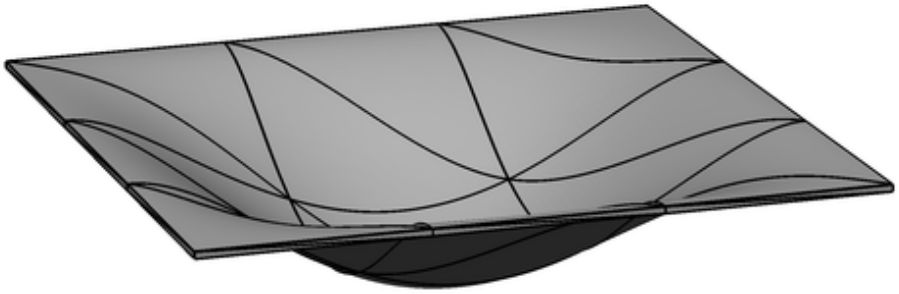

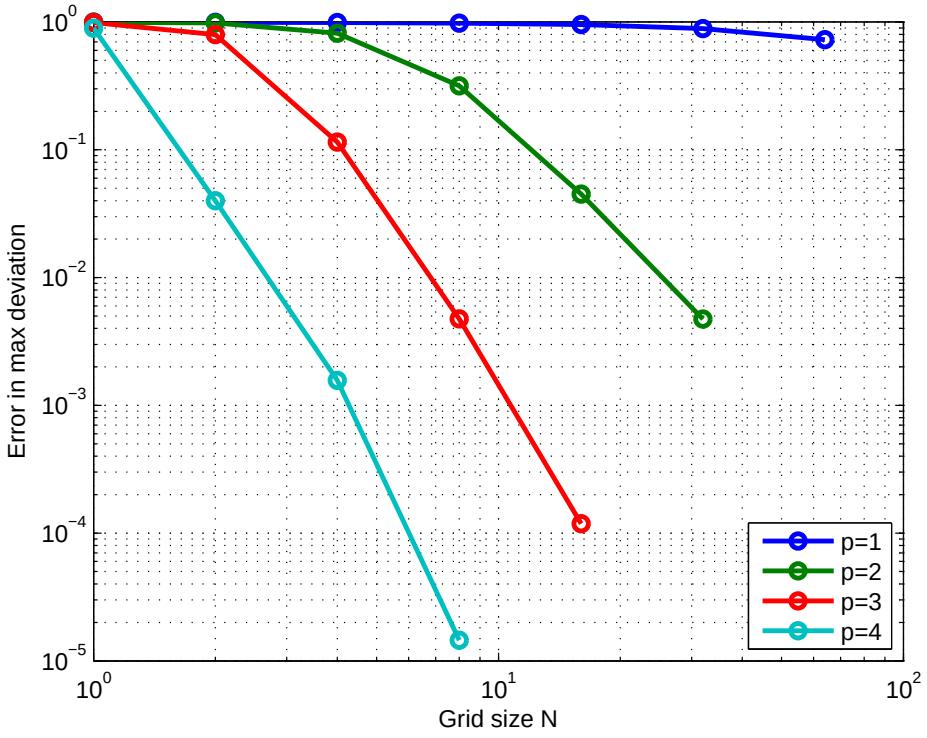

Example: Airbag Inflation

- Undeformed configuration: Two thin sheets, attached at the edges (thickness=10^{-3}, diagonal=1.2)
- Discretize with stretched tetrahedra and high-order DG elements
- Interior pressure p_0 applied at $t = 0$, quasi-static evolution

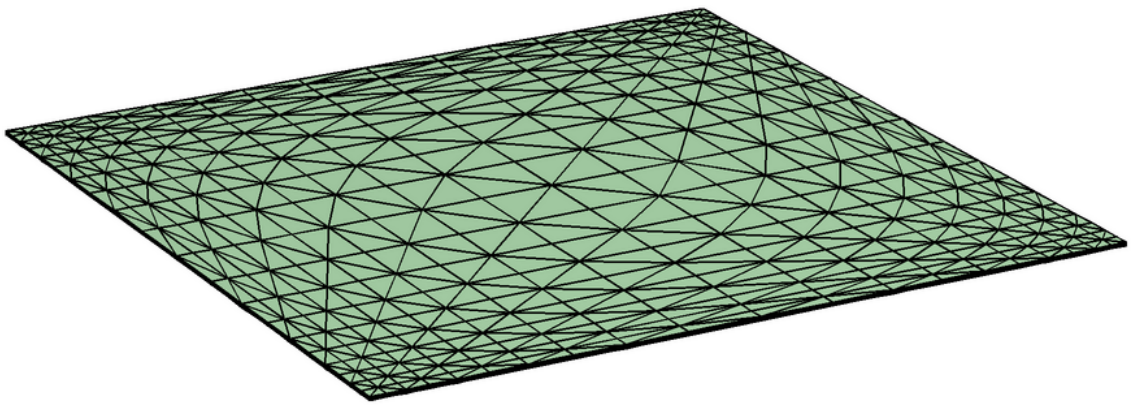

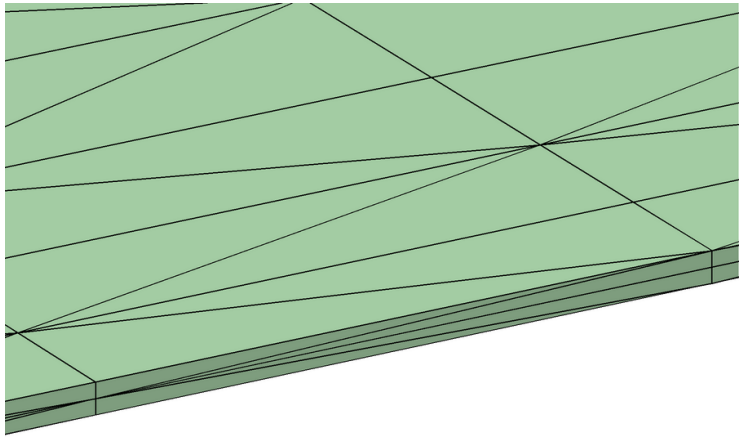

Example: Airbag Inflation

- 40-by-40 grid, 16000 tetrahedra, polynomial order $p = 3$
- No specialized membrane models required
- Hard to define convergence, but $\max(\Delta z) \rightarrow$ fixed value

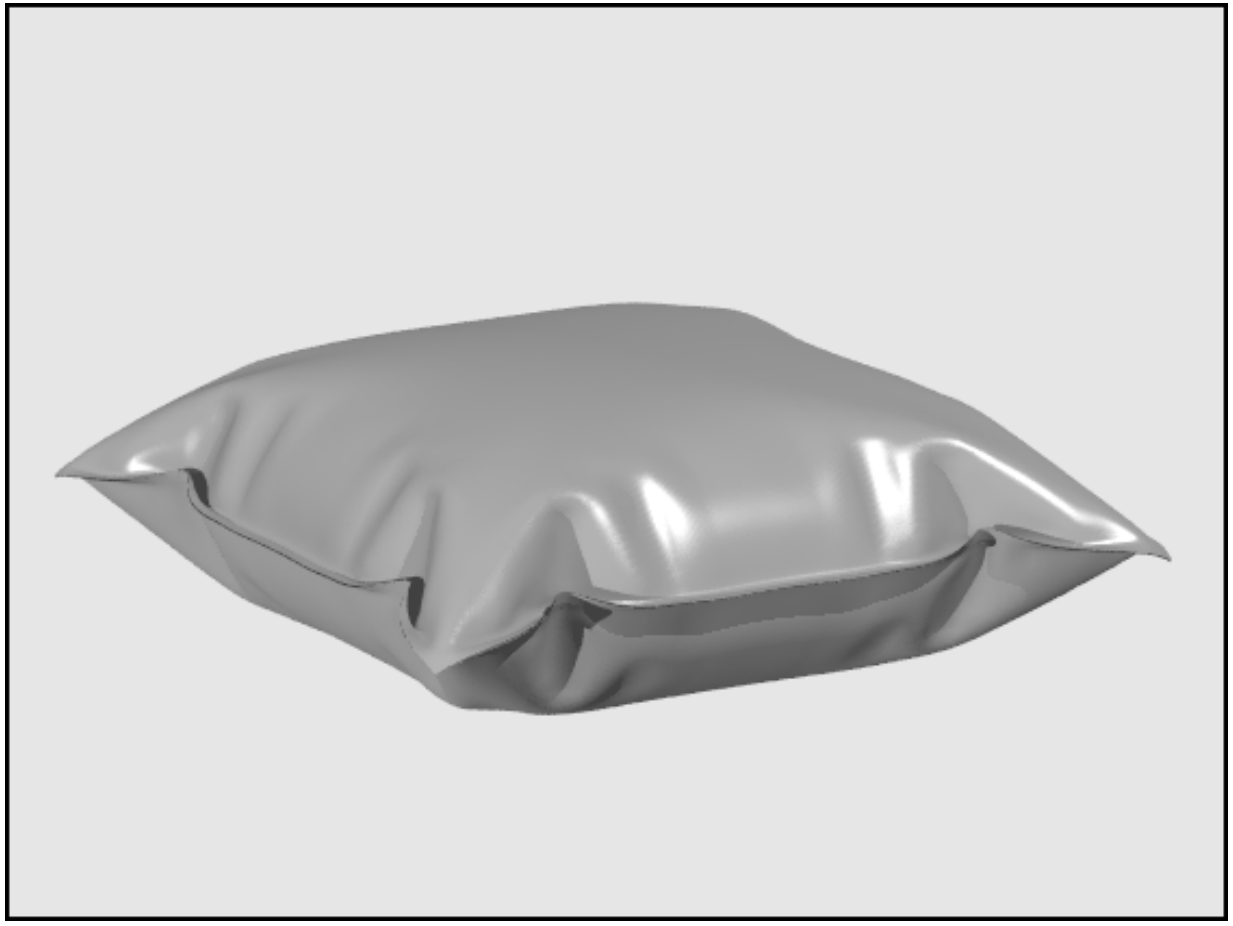

Volumetric Modeling of Coupled Beam/Membrane

- No modeling required to couple beams/membranes
- Only a question of generating the stretched tetrahedral meshes

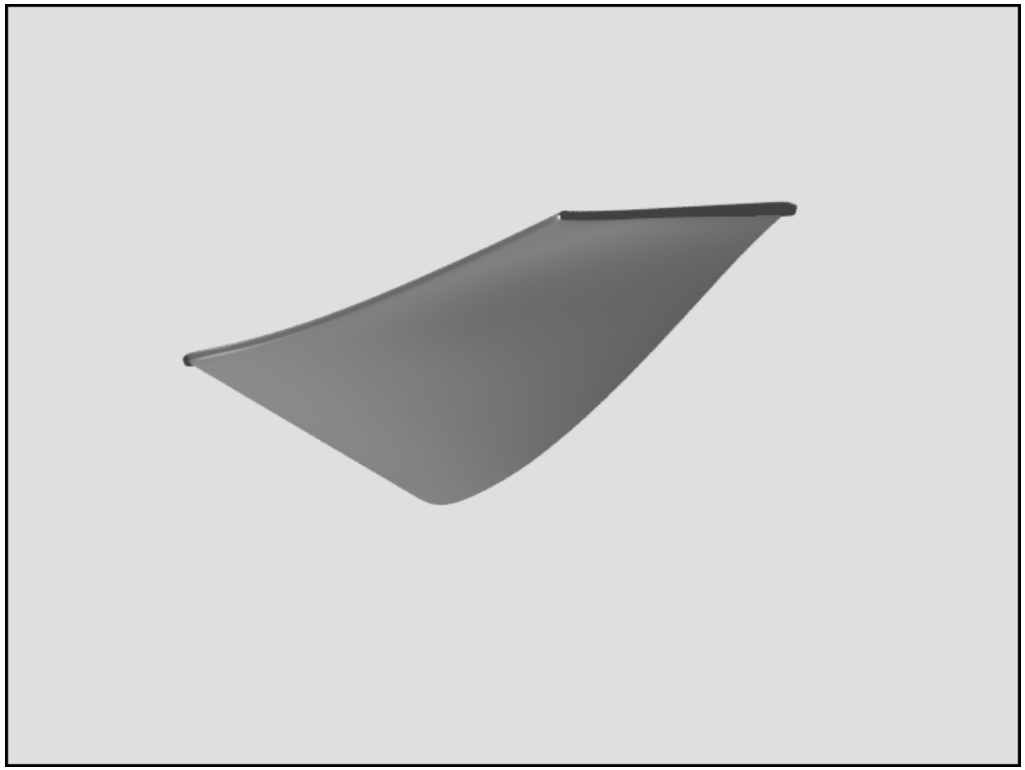

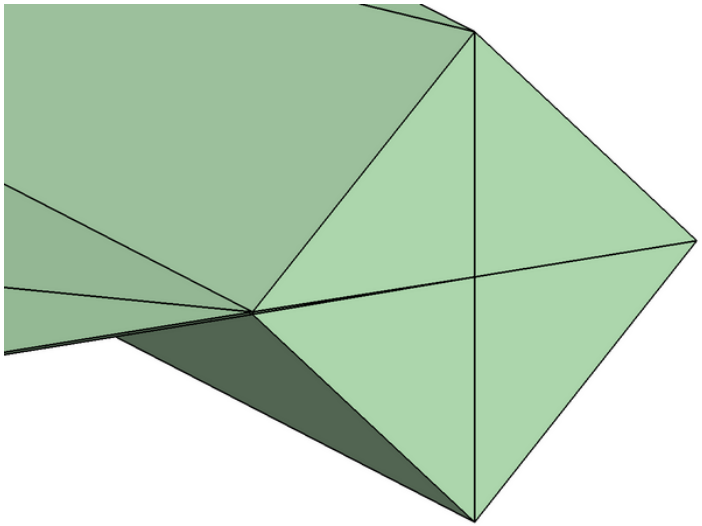

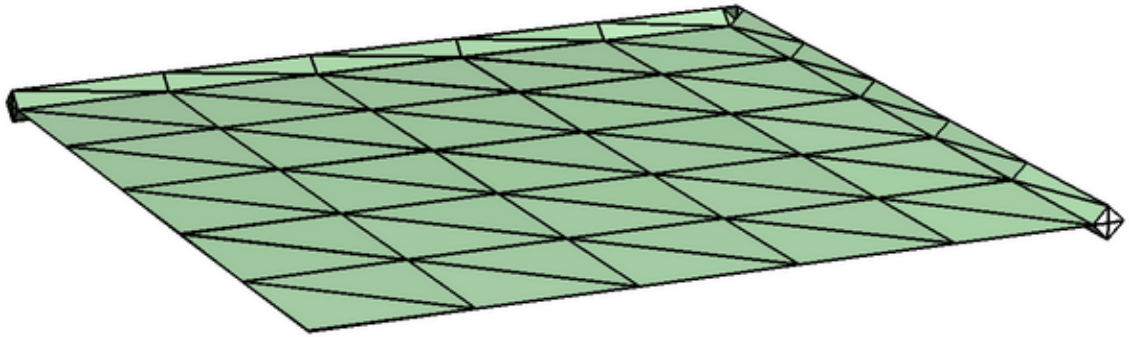

J2 Viscoplasticity

- Formulate J2 Viscoplasticity model as system of equations
- *Systematic discretizations* which converge under h/p refinement
- *Arbitrary orders of accuracy* in space and time

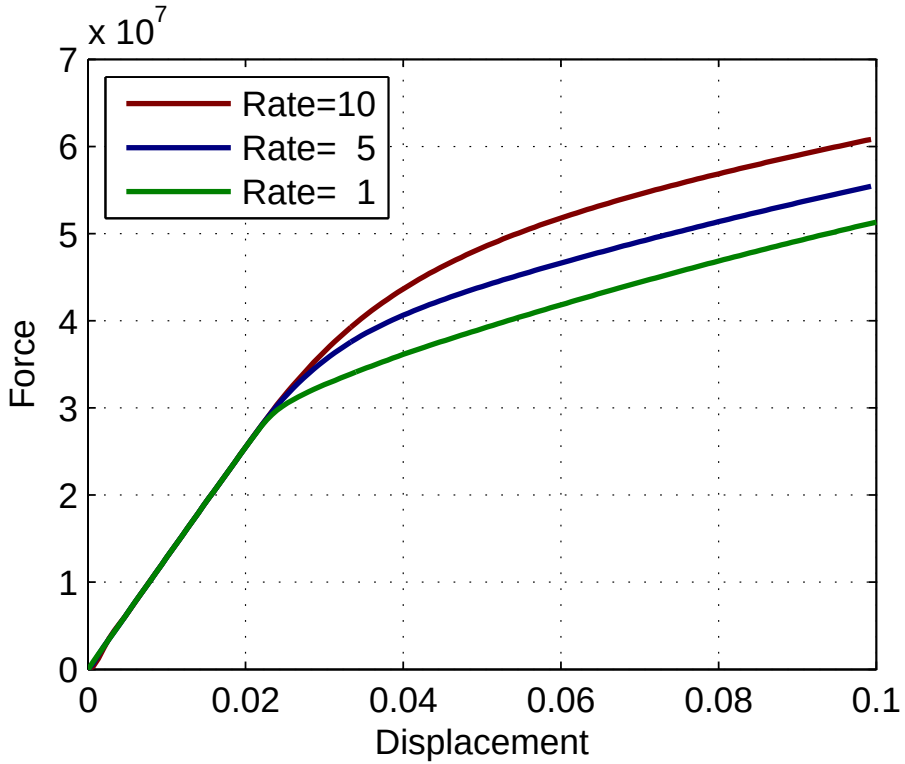

Rate = 1

Rate = 10

J2 Viscoplasticity as System of Equations

- Introduce the *scalar plastic deformation* ϵ_p and the *right plastic Cauchy-Green tensor* $\boldsymbol{C}_p$ as unknowns

$$\mathcal{U} = \begin{pmatrix} \boldsymbol{x} & \boldsymbol{p} & \epsilon_p & \boldsymbol{C}_p \end{pmatrix}$$

- Evolution equations for $\boldsymbol{x}, \boldsymbol{p}$ similar to before:

$$\dot{\boldsymbol{x}} = \boldsymbol{p}/\rho_0$$
$$\dot{\boldsymbol{p}} - \nabla \cdot \boldsymbol{P} = \rho_0 \boldsymbol{b}$$

where

$$\boldsymbol{P} = \mu(\boldsymbol{b}_e \boldsymbol{F}^{-T} - \boldsymbol{F}^{-T}) + \lambda(\ln J_e)\boldsymbol{F}^{-T},$$
$$J_e = \sqrt{|\boldsymbol{b}_e|}, \quad \boldsymbol{b}_e = \boldsymbol{F}\boldsymbol{C}_p^{-1}\boldsymbol{F}^T$$

J2 Viscoplasticity as System of PDEs/ODEs

- Evolution equations for ϵ_p and $\boldsymbol{C}_p$:

$$\dot{\epsilon}_p = \frac{1}{\eta}\langle \bar{\tau} - \tau_y(\epsilon_p)\rangle$$

$$\dot{\boldsymbol{C}}_p = \frac{3}{\eta/\mu}\frac{\langle \bar{\tau} - \tau_y(\epsilon_p)\rangle}{\bar{\tau}}\left(\boldsymbol{F}^T\boldsymbol{F} - \frac{1}{3}(tr\boldsymbol{b}_e)\boldsymbol{C}_p\right)$$

where η is a viscosity parameter, $\langle\cdot\rangle$ is the ramp function, and

$$\boldsymbol{\tau} = \boldsymbol{P}\boldsymbol{F}^T = \mu(\boldsymbol{b}_e - \boldsymbol{I}) + \lambda(\ln J_e)\boldsymbol{I}$$

$$\boldsymbol{\tau}' = \boldsymbol{\tau} - \frac{1}{3}(tr\boldsymbol{\tau})\boldsymbol{I} = \mu(\boldsymbol{b}_e - \frac{1}{3}(tr\boldsymbol{b}_e)\boldsymbol{I})$$

$$\bar{\tau} = \sqrt{\frac{3}{2}\boldsymbol{\tau}' : \boldsymbol{\tau}'}$$

$$\tau_y = \tau_y^0 + H\epsilon_p$$

Example: Strain Localization

- With *strain softening* ($H < 0$), deformations localize in narrow bands of intense straining
- Sharp jumps in displacements, location unknown a priori
- Insensitive to mesh with $p > 2$

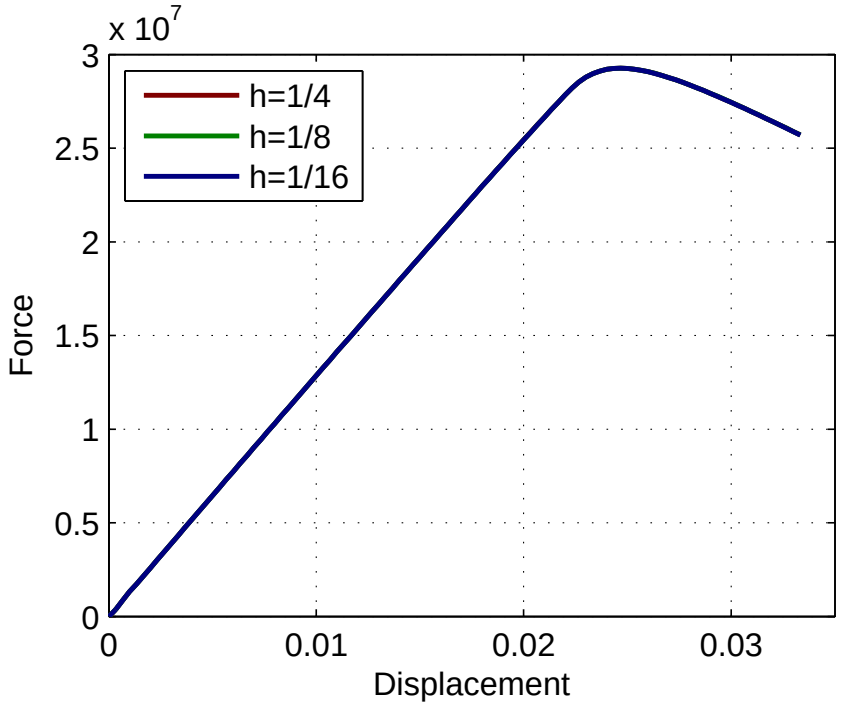

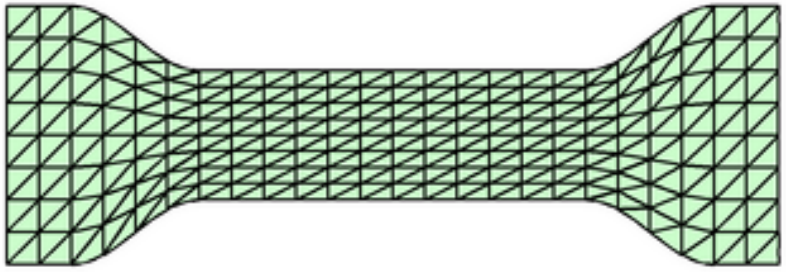

Mesh, $p = 4$

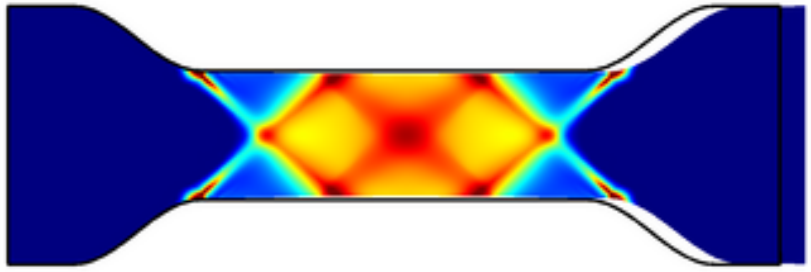

Plastic deformation ϵ_p

Conclusions

- Important steps toward practical DG solver for realistic problems:
  - Efficient viscous discretization (the CDG method)
  - General purpose multigrid/block ILU preconditioner
  - Robustness by sensors and artificial viscosity, for RANS and shocks
  - Optimal accuracy for deformable domains by mapping approach
  - High order Lagrangian DG formulations for solid dynamics
- Current work: Full monolithic DG fluid-structure formulation, improved numerical schemes and algorithms, 3-D curved mesh generation, extensions for LES/DES, applications in flapping flight, aeroacoustics, instabilities in solids, and supersonic flows